



AN ANALYSIS METHOD FOR DOUBLE PERIODIC  
NONPLANAR ANTENNA ARRAYS

THESIS

Presented in Partial Fulfillment of the Requirements for  
the degree Master of Science in the Graduate  
School of The Ohio State University

by

Robert Andre, B.S.

\*\*\*\*\*

The Ohio State University

1985

DISTRIBUTION STATEMENT A

Approved for public release  
Distribution Unlimited

Master's Examination Committee:

Benedikt A. Munk

Edward K. Damon

Approved By

Adviser

Department of Electrical Engineering

19950925 109

DTIC QUALITY INSPECTED 8

Accesion For	
NTIS	CRA&I
DTIC	TAB
Unannounced	
Justification	
By <i>Benedikt Andre</i>	
Distribution /	
Availability Codes	
Dist	Avail and/or Special
A-1	

THESIS ABSTRACT

THE OHIO STATE UNIVERSITY  
GRADUATE SCHOOL

NAME: Andre, Robert

QUARTER/YEAR: Fall 1985

DEPARTMENT: Electrical Engineering

DEGREE: M.Sc.

ADVISER'S NAME: Benedikt A. Munk

TITLE OF THESIS: An Analysis Method for Doubly Periodic Nonplanar  
Antenna Arrays

The self impedance of a doubly periodic phased antenna array is a necessary quantity for the calculation of the scattering and transmitting behavior of the phased array. Previous work has shown a straightforward method of performing this impedance calculation when all the elements lie within the plane of the array. For nonplanar elements, this procedure produces complex and computationally undesirable equations. By introducing a three-dimensional array and using symmetry considerations, the nonplanar problem may be changed to a simpler planar one. This method enables the calculation of mutual and self impedances for a wide class of complex current distribution.

  
Adviser's Signature

## TABLE OF CONTENTS

LIST OF FIGURES	iii
<u>CHAPTER</u>	<u>PAGE</u>
I. INTRODUCTION	1
A. BACKGROUND	1
B. OVERVIEW	4
C. THE END OF COORDINATES	8
II. THE COORDINATE FREE PLANE WAVE EXPANSION	10
A. TWO-DIMENSIONAL ARRAYS	10
B. THREE-DIMENSIONAL VOLUME ARRAYS	16
C. IMPEDANCE EQUATIONS FOR WIRE ANTENNAS	22
D. THE EXCITATION VECTOR $\vec{s}$	26
III. THE NONPLANAR IMPEDANCE	28
A. GENERAL CONSIDERATIONS	28
B. DIPOLE ARRAY	30
C. LOOP ARRAY	34
IV. CONCLUSION	48
APPENDICES	
A DERIVATION OF THE FIELDS FROM A PLANAR ARRAY	49
Evaluating $G(R)$	51
The Electric and Magnetic Fields	55
B PATTERN FACTORS FOR DIPOLES AND LOOPS	57
Dipole Current	59
Loop Current	62
BIBLIOGRAPHY	65

## LIST OF FIGURES

1.1. Standard form of rectangular lattice of antenna elements.	2
1.2. The field generated by this nonplanar array takes a different form in each of these three regions.	2
1.3. Side view of $\hat{y}$ oriented nonplanar dipole array with interelement spacing $D_x$ , $D_z$ .	5
1.4. Volume array formed by adding an infinite number of identical dipole arrays with interplanar spacing $D_y$ .	5
2.1. An array of antenna elements defined by the direct lattice vectors $\vec{d}_1$ and $\vec{d}_2$ .	11
2.2. Lattice rows corresponding to the covariant reciprocal lattice vector $\vec{b}^1$ . Each vector in the reciprocal lattice has a corresponding row structure in the direct lattice.	13
2.3. Volume array formed by the three lattice vectors $\vec{D}_1, \vec{D}_2, \vec{D}_e$ . The reciprocal lattice vector $\vec{b}^3$ is orthogonal to the $\vec{D}_1, \vec{D}_2$ plane and of unit length.	17
3.1. Single dipole used in the example.	30
3.2. Incident angle parameters $\alpha$ and $n$ .	32
3.3. Scan impedance for an array of $\hat{y}$ directed dipoles for various angles of incidence and frequencies.	33

AQ495-1392

R. C. HANSEN, INC.

R. C. Hansen, Ph.D., D.Eng.(hon), FIEE, FIEEE

(818) 345-0770  
FAX 345-1259  
Home 345-5917

P.O. BOX 570215  
Tarzana, CA 91357

# 7 LOAN DOCUMENT

4 June 1995

4 June 1995

ATTN: DTIC/OCP (Joyce Charis)  
Defense Technical Information Center  
Cameron Station  
Alexandria, VA 22304-6145

Dear Joyce,

Enclosed is the report, OSU 715582, Thesis by R. Andre, we discussed over the phone. We have decided that we would like to lend this report to DTIC. When you have made your copies please return the report to the following address:

R. C. Hansen, Inc.  
P.O. Box 570215  
Tarzana, CA 91357-0215

Thank you for your assistance.

Sincerely yours,

Bob Hansen

Robert C. Hansen

RCH:1s

**Enclosure**

User Code: 21589

NTIS Deposit Account Number: 78146-8

3.4. Example of mutual impedance calculations.	35
3.5. Mutual impedance between $\hat{y}$ directed dipole arrays with separation $0_y=0.0, 0_z=0.2$ .	36
3.6. Mutual impedance between $\hat{y}$ directed dipole arrays with separation $0_y=0.0, 0_z=0.35$ .	37
3.7. Mutual impedance between $\hat{y}$ directed dipole arrays with separation $0_y=0.0, 0_z=0.5$ .	38
3.8. Mutual impedance between $\hat{y}$ directed dipole arrays with separation $0_y=-0.5, 0_z=0.5$ .	39
3.9. Mutual impedance between $\hat{y}$ directed dipole arrays with separation $0_y=-1.0, 0_z=0.5$ .	40
3.10. Single row of loop antennas etched on a copper clad pc board with interelement spacing $\ D_1\ $ . Rotation angle $\theta$ is used in the example.	41
3.11. Nonplanar array formed by stacking pc boards.	41
3.12. Stacked pc boards seen edge on and rotated by the angle $\phi$ .	43
3.13. With $\theta=0$ and $\phi=0$ , only the edge of the loops can be seen looking down onto the hexagonal lattice.	43
3.14. Self impedance for a loop array with $\theta=0^\circ$ and $\phi=0^\circ$ .	44
3.15. Self impedance for a loop array with $\theta=45^\circ$ and $\phi=0^\circ$ .	45
3.16. Self impedance for a loop array with $\theta=0^\circ$ and $\phi=45^\circ$ .	46

3.17. Self impedance for a loop array with $\theta=45^\circ$ and $\phi=45^\circ$ .	47
B.1. A linear round wire with a current distribution $\hat{p}I(\ell')$ .	58
B.2. Scattering (cosine) current distribution on a dipole.	60
B.3. Transmitting (sine) current distribution on a dipole.	62
B.4. Rectangular loop antenna.	63

## CHAPTER I

### INTRODUCTION

#### A. BACKGROUND

The analysis of doubly periodic phased antenna arrays has been well documented over the years. However, these studies have generally been limited to elements which lie completely within the plane of the array, referred to here as a totally planar array. There is a good reason for this. The nonplanar array, or a two-dimensional array with elements not within the plane of the array, is much more difficult to analyze due to the complexity of the self/mutual impedance terms. The need for greater flexibility in design has resulted in the recent study of arbitrarily oriented dipoles by English [1], nonplanar loop antennas by Kent [2], "V" dipoles by Lin [3], and the Clavin element by Ng [4].

The difficulties involved can be seen by considering a single nonplanar array in free space shown in Figure 1.1. A side view is shown in Figure 1.2. English identifies three regions of space: Region 1 contains only left going plane waves, Region 2 contains both left and right going waves, and Region 3 contains only right going plane waves. The induced voltage measured at the terminals of an antenna element (2) due to the field  $\vec{E}^{(1)}$  generated by the antenna array (1) is given by

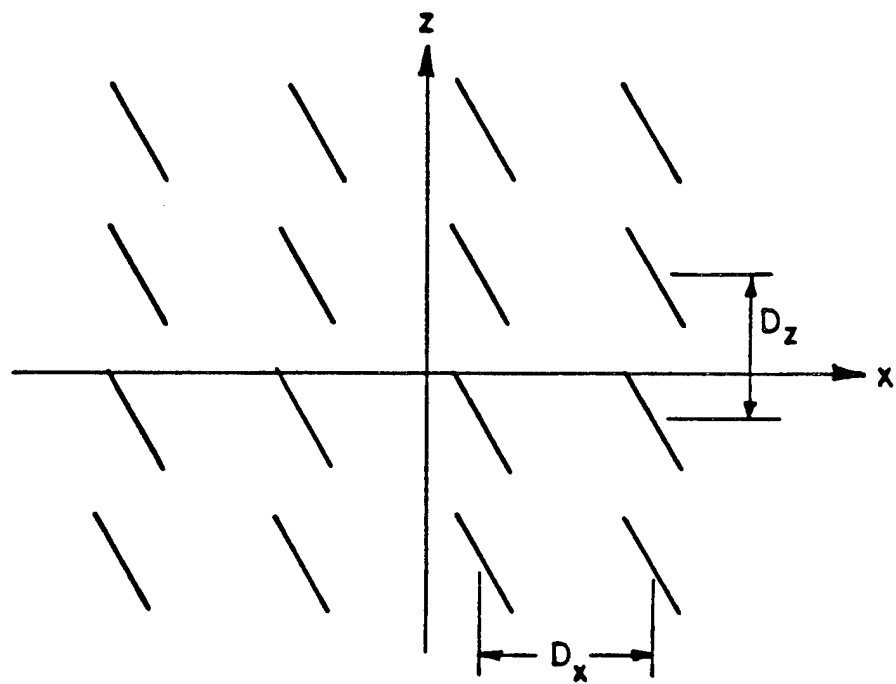


Figure 1.1. Standard form of rectangular lattice of antenna elements.

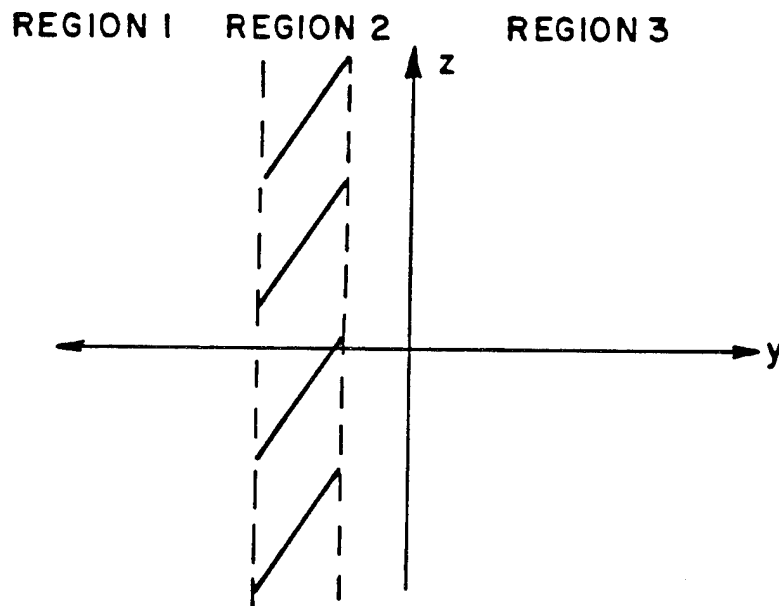


Figure 1.2. The field generated by this nonplanar array takes a different form in each of these three regions.

$$V^{2,1} = \frac{1}{I^{(2)t}} \int_{\text{element 2}} \vec{I}^{(2)t}(\vec{R}') \cdot \vec{E}^{(1)}(\vec{R}') d\vec{R}' \quad (1.1)$$

where  $\vec{I}^{(2)t}(\vec{R}')$  is the surface current distribution on antenna (2) under transmitting conditions,  $I^{(2)t}$  is the current magnitude at the terminals, and  $\vec{E}^{(1)}(\vec{R})$  is the field generated by the array. The mutual impedance between the antenna array (1) and test element (2) is

$$Z^{2,1} = -\frac{V^{2,1}}{I^{(1)}}. \quad (1.2)$$

When the test element (2) and the reference element (1) of the array are the same, Equation (1.2) gives the self impedance of the phased array. In order to find this self impedance, the field next to the elements, in Region 2, must be known. Region 2 fields contain left and right-going waves which depend on both the source point and observation point. The impedance calculation involves one integration over the current sources to produce the field  $\vec{E}^{(1)}(\vec{R})$  and another integration over the test element current distribution  $I^{(2)t}(\vec{R})$  of Equation (1.1). The resulting expressions for a nonplanar array involve tedious iterated integrals. With a totally planar array, the integrals are independent and may be separated.

Besides the complexity, these self impedance equations no longer have the rapidly decaying exponential term which guarantees fast convergence of the doubly infinite summation. This means longer computer run time.

With dielectric layers added, English showed that the self impedance of an array may be decomposed into five modes,

$$Z_{\text{self}} = Z_1 + Z_2 + Z_3 + Z_4 + Z_5 . \quad (1.3)$$

Modes two thru five are the four bounce modes which exist because of the dielectric boundaries. These modes use the same pattern factors and have the same form for nonplanar as for planar arrays. Mode one is the direct mode and is the self impedance of the array embedded in a homogeneous space with dielectric constants  $\epsilon_r$  and  $\mu_r$ . This report presents a method for finding the self impedance of a nonplanar array in a homogeneous space which can be combined with the four bounce mode impedances to find the total impedance of a nonplanar array in a stratified dielectric medium. Dielectric layers will no longer be considered here; all arrays will reside in a homogeneous medium.

## B. OVERVIEW

The typical geometry for a single nonplanar array, as shown in Figure 1.1, consists of a rectangular lattice in the x-z plane with interelement spacings  $D_x$  and  $D_z$ . Skewed grids in the x-z plane have also been examined by Kornbau [5]. As an example, consider the array of  $\hat{y}$  oriented dipoles in Figure 1.3 and denote the self impedance of this array by  $Z_0(D_x, D_z)$ . We wish to find this self impedance. This example will show the intuitive concepts of the method to be presented in the following chapters and provide a first look at the specialized notation involved.

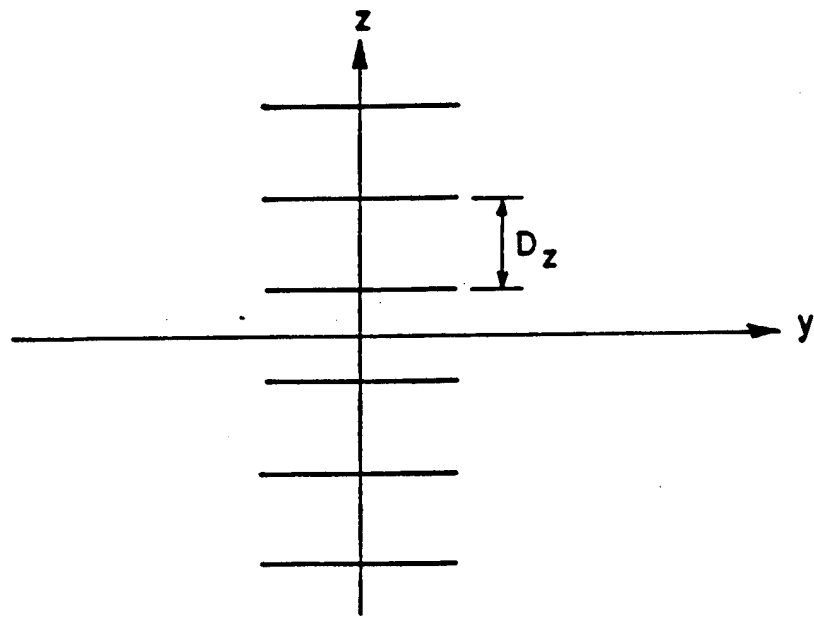


Figure 1.3. Side view of  $\hat{y}$  oriented nonplanar dipole array with interelement spacing  $D_x$ ,  $D_z$ .

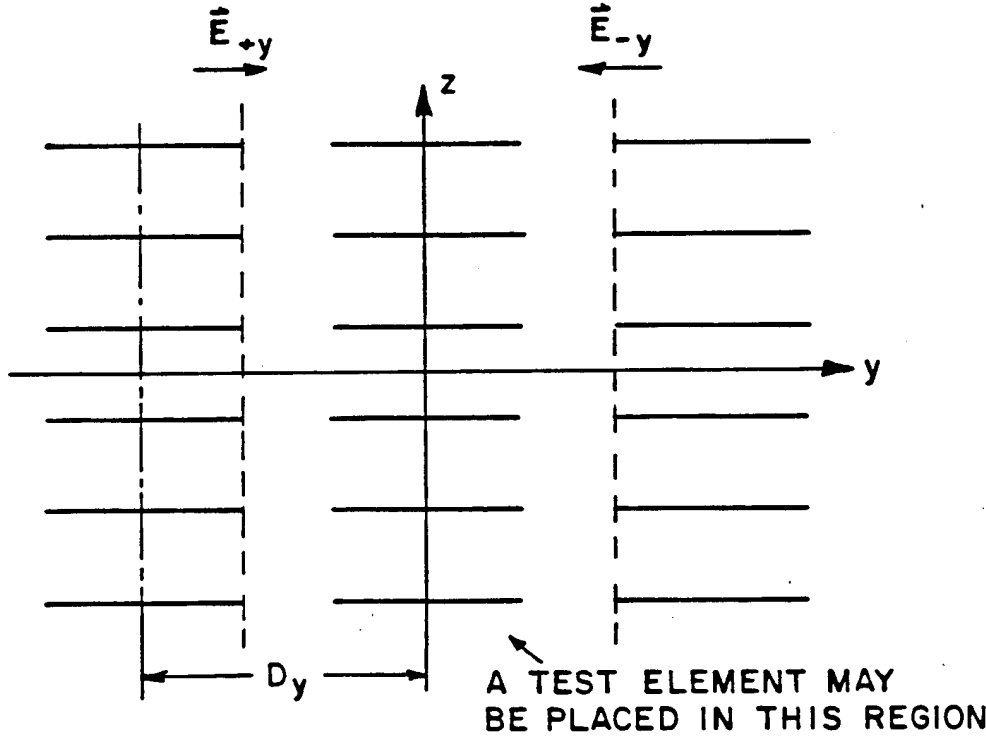


Figure 1.4. Volume array formed by adding an infinite number of identical dipole arrays with interplanar spacing  $D_y$ .

We begin by adding an infinite number of identical nonplanar arrays with interplanar spacing  $D_y$  so as to form a volume array as shown in Figure 1.4. The spacing  $D_y$  should be larger than the total dipole length. The field around our original two-dimensional dipole array can be divided into three parts:  $\vec{E}_0$  due to the original array,  $\vec{E}_{+y}$  due to the left half-infinite volume of dipoles, and  $\vec{E}_{-y}$  due to the right half-infinite volume of dipoles.  $\vec{E}_{+y}$  and  $\vec{E}_{-y}$  are right going and left going plane waves respectively. This field may be integrated over a test element in Equation (1.1) to find the volume impedance,

$$Z_{\text{volume}} = Z_0(D_x, D_z) + Z_{+y}(D_x, D_z | D_y) + Z_{-y}(D_x, D_z | D_y). \quad (1.4)$$

$Z_0(D_x, D_z)$  is still unknown. However,  $Z_{+y}$  and  $Z_{-y}$  may be easily calculated because the test element is not within the regions which generate  $\vec{E}_{+y}$  and  $\vec{E}_{-y}$ . There is another way of calculating  $Z_{\text{volume}}$ . This volume array is equivalent to an infinite number of planar arrays, all parallel to the  $x$ - $y$  plane, extending into the  $\hat{z}$  direction. In the  $\hat{x}$ - $\hat{y}$  plane, our  $\hat{y}$  directed dipoles form a totally planar array with a self impedance  $Z_0(D_x, D_y)$  which may be readily evaluated by standard methods. Also,  $Z_{+z}$  and  $Z_{-z}$  can be calculated to form

$$Z_{\text{volume}} = Z_0(D_x, D_y) + Z_{+z}(D_x, D_y | D_z) + Z_{-z}(D_x, D_y | D_z). \quad (1.5)$$

Subtracting Equation (1.4) from Equation (1.5) gives

$$Z_0(D_x, D_z) - Z_0(D_x, D_y) = Z_\Delta(D_x | D_z + D_y) \quad (1.6)$$

with

$$\begin{aligned} Z_\Delta(D_x | D_z + D_y) &= Z_{+z}(D_x, D_y | D_z) + Z_{-z}(D_x, D_y | D_z) \\ &- Z_{+y}(D_x, D_z | D_y) - Z_{-y}(D_x, D_z | D_y). \end{aligned} \quad (1.7)$$

Equation (1.6) shows how to find the nonplanar self impedance  $Z_0(D_x, D_z)$ ; we calculate the planar self impedance  $Z_0(D_x, D_y)$  and the difference impedance  $Z_\Delta(D_x | D_z + D_y)$  and add. The critical point in this procedure is that the dipole has maintained the same  $\hat{y}$  orientation throughout. This means that the vector pattern functions

$$\hat{p}(\hat{r}) = \frac{1}{I(\hat{R}^{(1)})} \int_{\text{element}} \hat{I}(\hat{R}') e^{j\beta\hat{R}' \cdot \hat{r}} d\hat{R}' \quad (1.8)$$

which find their way into the impedance equations and which depend only upon element orientation, are the same in every impedance term. The changing lattices have their effect on the argument  $\hat{r}$  and not on the pattern function.

For this example of a  $\hat{y}$  directed dipole, we transformed the planar lattice from the  $\hat{x}-\hat{z}$  plane in which the element is nonplanar to the  $\hat{x}-\hat{y}$  plane where the element is planar and related the two self impedances by Equation (1.6). For an arbitrarily oriented dipole with direction  $\hat{p}$ ,

we would like to be able to transform our lattice from the  $\hat{x}$ - $\hat{z}$  plane to the  $\hat{z}$ - $\hat{p}$  plane since this plane allows us to easily calculate the self impedance of the totally planar  $\hat{p}$  directed dipoles. In order to relate the self impedance of the dipoles in the  $\hat{x}$ - $\hat{z}$  lattice to the self impedance in the  $\hat{z}$ - $\hat{p}$  lattice, we form a three-dimensional  $\hat{x}$ - $\hat{z}$ - $\hat{p}$  volume lattice ( $\hat{x}$ ,  $\hat{z}$ , and  $\hat{p}$  are assumed to be linearly independent). This intermediate volume array enables us to write

$$Z_0(D_x, D_z) = Z_0(D_z, \hat{p}) + Z_\Delta(D_z | D_x + \hat{p}) \quad (1.9)$$

in which the terms on the right are easily evaluated by methods which will be developed in Chapter II. Chapter III will examine this example in more detail. By changing the lattice, we shall see how to find the self and mutual impedances of much more complex structures.

### C. THE END OF COORDINATES

The plane wave expansion of the fields from a periodic surface began with a rectangular lattice. A rectangular coordinate system of unit vectors  $\hat{x}, \hat{y}, \hat{z}$  was therefore the natural basis for expanding vectors. With the introduction of skewed lattices, the same rectangular coordinates were used with little difficulty even though they are not the most natural basis vectors. Using the method in this report, however, an antenna element may only be planar in a skewed plane which does not contain any of the three coordinate axes  $\hat{x}, \hat{y}$ , or  $\hat{z}$ . In order to calculate the planar impedance required by Equation (1.6), we must

either rotate the elements into the  $\hat{x}$ - $\hat{z}$  plane where we are most comfortable in calculating impedances, or adopt a different set of basis vectors for the plane wave expansion. The first alternative means giving up the invariance of the pattern function under a change in lattice while the second means adopting a more general theory of periodic structures. The choice is clear. By dropping the rectangular coordinate system we are able to see directly how a change in the lattice structure affects the physics of the plane wave expansion. Coordinate systems will only be used when it is necessary to consider specific examples in Chapter III.

Chapter II examines the coordinate free plane wave expansions in both two and three-dimensional lattices. The notation to be used for the direct and reciprocal lattices is chosen to remain consistent with the classic work by Leon Brillouin [6], Wave Propagation in Periodic Structures. This book is recommended for its practical insight into the mathematics of periodic structures.

CHAPTER II  
THE COORDINATE FREE PLANE WAVE EXPANSION

A. TWO-DIMENSIONAL ARRAYS

The Region 1 and Region 3 fields from a periodic two-dimensional array of current sources is derived in Appendix A. The array lattice, often referred to as the direct lattice, is defined by the two vectors  $\vec{d}_1$  and  $\vec{d}_2$  shown in Figure 2.1. The reference point or terminals for the  $q, m$  current source is located at

$$\vec{R}_{qm} = q\vec{d}_1 + m\vec{d}_2 + \vec{r}^{(1)}. \quad (2.1)$$

We assume that the currents at each lattice point are identical except for a linear phase difference of the form  $e^{-j\beta s \cdot \hat{R}_{qm}}$ . Equation (A.40) gives the electric field,

$$\vec{E}^{(1)}(\vec{R}) = \frac{z_c I^{(1)}(\vec{R}^{(1)})}{2\pi \vec{d}_1 \times \vec{d}_2} \sum_{n=-\infty}^{\infty} \sum_{k=-\infty}^{\infty} \frac{e^{-j\beta(\vec{R}-\vec{R}^{(1)}) \cdot \hat{r}_{\pm}}}{r_3} \left[ (\vec{p}^{(1)}(\hat{r}_{\pm}) \times \hat{r}_{\pm}) \times \hat{r}_{\pm} \right] \quad (2.2)$$

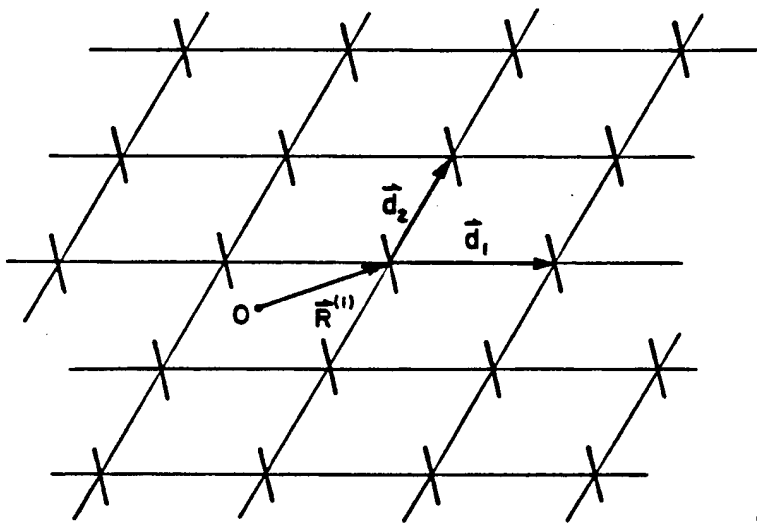


Figure 2.1. An array of antenna elements defined by the direct lattice vectors  $\vec{d}_1$  and  $\vec{d}_2$ .

with

$$Z_C = \sqrt{\frac{\mu}{\epsilon}} \quad (2.3)$$

$$\hat{p}^{(1)}(\hat{r}) = \frac{1}{I^{(1)}(\hat{R}^{(1)})} \int_{\text{element 1}} I^{(1)}(\hat{R}') e^{j\beta\hat{R}' \cdot \hat{r}} d\hat{R}' . \quad (2.4)$$

$\hat{R}'$  is a vector from  $\hat{R}^{(1)}$  to the integration point. The propagation vector  $\hat{r}$  is expanded on the special basis  $\{\hat{b}^j\}$  which forms the reciprocal lattice,

$$\hat{r}_{\pm} = r_1 \hat{b}^1 + r_2 \hat{b}^2 \pm r_3 \hat{b}^3 \quad (2.5)$$

$$r_1 = s_1 + k\lambda \quad s_1 = \hat{s} \cdot \vec{d}_1 \quad (2.6)$$

$$r_2 = s_2 + n\lambda \quad s_2 = \hat{s} \cdot \vec{d}_2 \quad (2.7)$$

$$r_3 = \sqrt{1 - \|r_1\|^2 + \|r_2\|^2} \quad \text{evaluated in the fourth quadrant.} \quad (2.8)$$

Equations (2.2) - (2.8) have some features not found in the usual rectangular coordinate plane wave expansion which we will now examine.

Our original lattice provided us with only two vectors to describe three-dimensional space. Therefore, we may arbitrarily choose a third vector  $\vec{d}_3$  to form a three-dimensional basis  $(\vec{d}_1, \vec{d}_2, \vec{d}_3)$ . The simplest choice is the unit vector

$$\vec{d}_3 = \vec{d}_1 \times \vec{d}_2 / \|\vec{d}_1 \times \vec{d}_2\|. \quad (2.9)$$

The  $\{\vec{d}_i\}$  vectors of the direct lattice are also known as contravariant vectors and are a natural basis for expanding other contravariant vectors such as the position vector  $\vec{R}$ .

In periodic structures, there is another basis  $(\vec{b}^1, \vec{b}^2, \vec{b}^3)$  associated with the direct lattice and defined by

$$\vec{d}_i \cdot \vec{b}^j = \delta_i^j \quad (2.10)$$

where  $\delta_i^j$  is the Kronecker delta. The  $\{\vec{b}^j\}$  vectors are the corresponding covariant vectors and are the most natural basis for expanding propagation vectors such as  $\vec{r}$  in Equations (2.5) - (2.8) and the incident vector direction  $\hat{s}$ ,

$$\hat{s} = s_1 \vec{b}^1 + s_2 \vec{b}^2 + s_3 \vec{b}^3 \quad (2.11)$$

$$s_i = \hat{s} \cdot \vec{d}_i \quad (2.12)$$

The lattice defined by  $\vec{b}^1$  and  $\vec{b}^2$  is the reciprocal lattice and is usually referred to as k-n space because of Equations (2.5) - (2.7).

While the  $(\vec{d}_1, \vec{d}_2)$  vectors correspond to lattice points, the  $(\vec{b}^1, \vec{b}^2)$  vectors correspond to lattice rows as shown in Figure 2.2 where one reciprocal lattice vector  $\vec{b}'$  and its lattice rows are given. The vector  $\vec{b}'$  has a direction orthogonal to the rows and a magnitude inversely proportional to the separation between the rows. It is this correspondence with lattice rows which makes the reciprocal basis so appropriate for expanding propagation vectors.

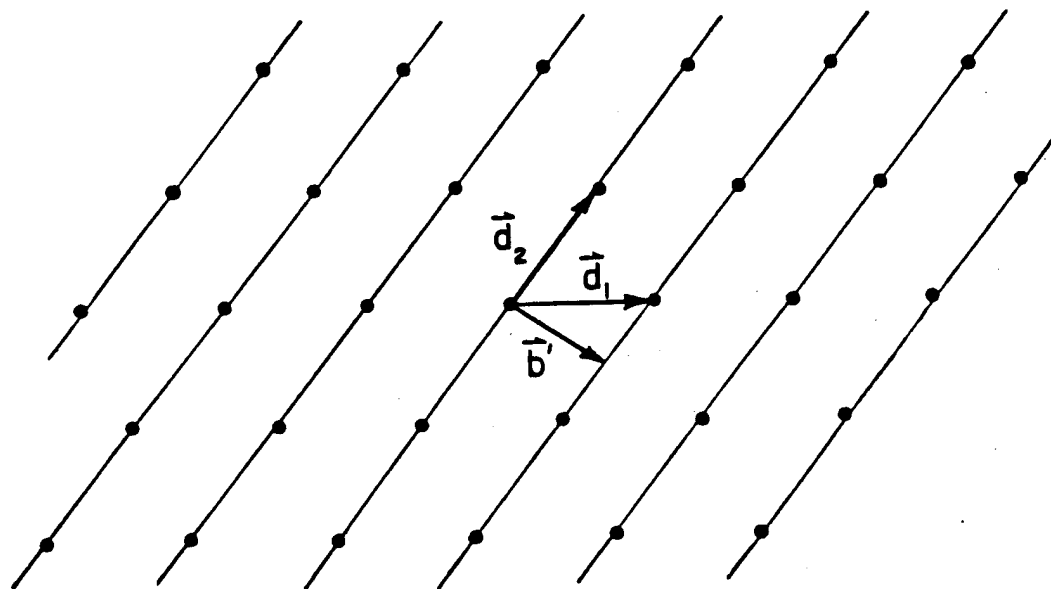


Figure 2.2. Lattice rows corresponding to the covariant reciprocal lattice vector  $\vec{b}'$ . Each vector in the reciprocal lattice has a corresponding row structure in the direct lattice.

Because of the simple geometry of the array, the convention of contravariant and covariant vectors is not really needed. The important concept is the way the plane wave spectrum of Equation (2.2) depends on the reciprocal lattice through  $\vec{r}$  in Equations (2.5) - (2.8).

The choice of  $\vec{d}_3$  in Equation (2.9) and the condition given in Equation (2.10) allows us to write

$$\begin{aligned}\vec{b}^1 &= \vec{d}_2 \times \vec{d}_3 / \|\vec{d}_1 \times \vec{d}_2\| \\ \vec{b}^2 &= \vec{d}_3 \times \vec{d}_1 / \|\vec{d}_1 \times \vec{d}_2\| \\ \vec{b}^3 &= \vec{d}_3 .\end{aligned}\tag{2.13}$$

As an example, consider the usual rectangular lattice

$$\begin{aligned}\vec{d}_1 &= D_x \hat{x} & \vec{d}_2 &= D_z \hat{z} \\ \hat{s} &= s_x \hat{x} + s_y \hat{y} + s_z \hat{z}.\end{aligned}\tag{2.14}$$

Then Equation (2.9) gives

$$\|\vec{d}_1 \times \vec{d}_2\| = D_x D_z\tag{2.15}$$

$$\vec{d}_3 = \hat{-y}.\tag{2.16}$$

The reciprocal lattice becomes,

$$\overset{\rightarrow}{b}^1 = 1/D_x \hat{x}$$

$$\overset{\rightarrow}{b}^2 = 1/D_z \hat{z} \quad (2.17)$$

$$\overset{\rightarrow}{b}^3 = -\hat{y} .$$

Equations (2.5) - (2.8) then give

$$s_1 = s_x D_x \quad s_2 = s_z D_z \quad (2.18)$$

$$r_1 = s_x D_x + k\lambda \quad r_2 = s_z D_z + n\lambda \quad (2.19)$$

$$r_1 \overset{\rightarrow}{b}^1 + r_2 \overset{\rightarrow}{b}^2 = \left[ s_x + k \frac{\lambda}{D_x} \right] \hat{x} + \left[ s_z + n \frac{\lambda}{D_z} \right] \hat{z} \quad (2.20)$$

$$r_3 = \sqrt{1 - \left[ s_x + k \frac{\lambda}{D_x} \right]^2 - \left[ s_z + n \frac{\lambda}{D_x} \right]^2} \quad (2.21)$$

$$\hat{r}_{\pm} = \left[ s_x + k \frac{\lambda}{D_x} \right] \hat{x} \pm r_3 \hat{y} + \left[ s_z + n \frac{\lambda}{D_x} \right] \hat{z} . \quad (2.22)$$

It is interesting to note that the switch to a coordinate free representation has replaced the  $D_x D_z$  term normally found in the denominator of Equation (2.2) with  $\|\overset{\rightarrow}{d}_1 \times \overset{\rightarrow}{d}_2\|$  which is the area of the parallelogram formed by the vectors  $\overset{\rightarrow}{d}_1$  and  $\overset{\rightarrow}{d}_2$ .

Equation (2.4) for the vector pattern function has the standard form since it is independent of the lattice.

## B. THREE-DIMENSIONAL VOLUME ARRAYS

Now consider a volume distribution of current sources defined by the direct lattice vectors  $\vec{D}_1$ ,  $\vec{D}_2$  and  $\vec{D}_e$  shown in Figure 2.3. The reference point is chosen to be at the origin for now. The field from the volume array will be found by summing the fields produced by the elements in the  $\vec{D}_1, \vec{D}_2$  planes. The reason for using the notation  $\vec{D}_e$  instead of  $\vec{D}_3$  for the third lattice vector is because the formulation will be based on the expansion of the previous section with

$$\vec{d}_1 = \vec{D}_1$$

$$\vec{d}_2 = \vec{D}_2$$

$$\vec{d}_3 = \vec{D}_1 \times \vec{D}_2 / \| \vec{D}_1 \times \vec{D}_2 \| .$$

The  $\vec{D}_1, \vec{D}_2$ , and  $\vec{D}_e$  vectors define the array while the  $\vec{d}_i$  and  $\vec{b}^j$  vectors act as local variables of the equations. Assume the currents have a plane wave type of phase difference but are otherwise periodic,

$$\vec{I}_{qml}^{(1)}(\vec{R}) = \vec{I}_{000}^{(1)}(\vec{R} - \vec{R}_{qml}) e^{-j\beta \vec{R}_{qml} \cdot \vec{s}} \quad (2.24)$$

where

$$\vec{R}_{qml} = q\vec{D}_1 + m\vec{D}_2 + l\vec{D}_e \quad (2.25)$$

and  $\vec{I}_{000}^{(1)}(\vec{R})$  is the current distribution of the reference element.

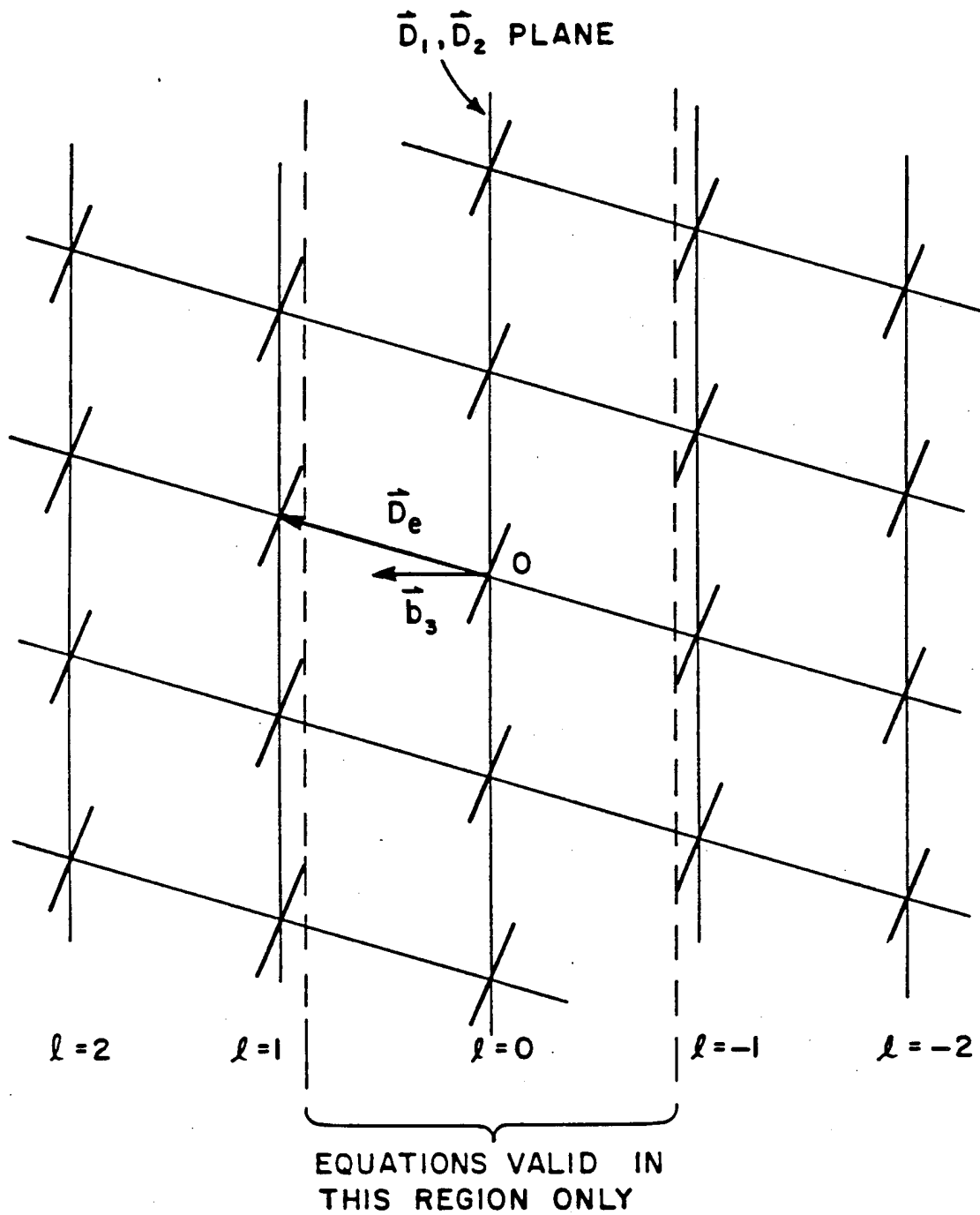


Figure 2.3. Volume array formed by the three lattice vectors  $\vec{D}_1, \vec{D}_2, \vec{D}_e$ .  
 The reciprocal lattice vector  $b^3$  is orthogonal to the  $D_1, D_2$  plane and is of unit length.

The volume array can be considered as an infinity of parallel planes with  $\vec{D}_1$  and  $\vec{D}_2$  as the planar lattice vectors and

$$\vec{R}_{00\ell} = \ell \vec{D}_e \quad (2.26)$$

as the reference point of the  $\ell$ th plane. The field from the  $\ell=0$  plane from Equation (2.2) is

$$\vec{E}_0^{(1)}(\vec{R}) = \frac{Z_c I_0}{2\pi \vec{D}_1 \times \vec{D}_2} \sum_{k=-\infty}^{\infty} \sum_{n=-\infty}^{\infty} \frac{e^{-j\beta R \cdot \hat{r}_{\pm}}}{r_3} [(\vec{P}^{(1)}(\hat{r}_{\pm}) \times \hat{r}_{\pm}) \times \hat{r}_{\pm}] \quad (2.27)$$

use + for  $\vec{R} \cdot (\vec{D}_1 \times \vec{D}_2) > 0$

- for  $\vec{R} \cdot (\vec{D}_1 \times \vec{D}_2) < 0$ .

The field from the  $\ell$ th plane is,

$$\vec{E}_{\ell}(\vec{R}) = E_0(R - \ell \vec{D}_e) e^{-j\beta \ell \vec{D}_e \cdot \vec{s}} \quad (2.28)$$

Therefore the total field is

$$\begin{aligned} \vec{E}^{(1)}(\vec{R}) &= \sum_{\ell=-\infty}^{-1} \vec{E}_{\ell}^{(1)}(R - \ell \vec{D}_e) e^{-j\beta \ell s_e} \\ &+ \vec{E}_0^{(1)}(\vec{R}) \\ &+ \sum_{\ell=1}^{\infty} \vec{E}_{\ell}^{(1)}(R - \ell \vec{D}_e) e^{-j\beta \ell s_e} \end{aligned} \quad (2.29)$$

with

$$s_e = \vec{s} \cdot \vec{D}_e . \quad (2.30)$$

We restrict  $\vec{R}$  to the region of validity between the  $\ell=-1$  and  $\ell=1$  planes; see Figure 2.3. Define

$$\sigma \equiv \text{sgn}(\vec{D}_e \cdot \vec{b}^3) \quad (2.31)$$

$$= \text{sgn}(\vec{D}_e \cdot (\vec{D}_1 \times \vec{D}_2)) . \quad (2.32)$$

Then Equation (2.29) may be written as

$$\begin{aligned} \vec{E}^{(1)}(\vec{R}) &= \sum_{\ell=-\infty}^{-1} \frac{Z_c I_0 e^{-j\beta \ell s_e}}{2 \|\vec{D}_1 \times \vec{D}_2\|} \sum_{k=-\infty}^{\infty} \sum_{n=-\infty}^{\infty} \frac{e^{-j\beta(\vec{R}-\ell\vec{D}_e) \cdot \hat{r}_{\sigma}}}{r_3} \\ &\quad [(\hat{P}^{(1)}(\hat{r}_{\sigma}) \times \hat{r}_{\sigma}) \times \hat{r}_{\sigma}] \\ &+ \vec{E}_0^{(1)}(\vec{R}) \\ &+ \sum_{\ell=1}^{\infty} \frac{Z_c I_0 e^{-j\beta \ell s_e}}{2 \|\vec{D}_1 \times \vec{D}_2\|} \sum_{k=-\infty}^{\infty} \sum_{n=-\infty}^{\infty} \frac{e^{-j\beta(\vec{R}-\ell\vec{D}_e) \cdot \hat{r}_{-\sigma}}}{r_3} \\ &\quad [(\hat{P}^{(1)}(\hat{r}_{-\sigma}) \times \hat{r}_{-\sigma}) \times \hat{r}_{-\sigma}] \end{aligned} \quad (2.33)$$

Rearranging summations gives terms of the form

$$\left[ \sum_{\ell=-\infty}^{\infty} e^{-j\beta\ell(s_e - \hat{D}_e \cdot \hat{r}_\sigma)} \right] \quad (2.34)$$

$$\left[ \sum_{\ell=1}^{\infty} e^{-j\beta\ell(s_e - \hat{D}_e \cdot \hat{r}_{-\sigma})} \right]. \quad (2.35)$$

Using the properties of the geometric series

$$\sum_{\ell=1}^{\infty} e^{-j\beta\ell x} = \frac{e^{-j\beta x}}{1-e^{-j\beta x}}, \quad (2.36)$$

Equation (2.33) may be simplified into the form

$$\vec{E}^{(1)}(\vec{R}) = \vec{E}_+^{(1)}(\vec{R}) + \vec{E}_0^{(1)}(\vec{R}) + \vec{E}_-^{(1)}(\vec{R}). \quad (2.37)$$

Moving the reference point to  $\vec{R}^{(1)}$  gives

$$\begin{aligned} \vec{E}_+^{(1)}(\vec{R}) &= \frac{Z_C I^{(1)}(\vec{R}^{(1)})}{2\pi \vec{D}_1 \times \vec{D}_2} \sum_{k=-\infty}^{\infty} \sum_{n=-\infty}^{\infty} \frac{e^{-j\beta(\vec{R}-\vec{R}^{(1)}) \cdot \hat{r}_\sigma}}{r_3} \cdot \\ &\quad \frac{e^{-j\beta(\hat{r}_\sigma \cdot \vec{D}_e - s_e)}}{1-e^{-j\beta(\hat{r}_\sigma \cdot \vec{D}_e - s_e)}} [(\vec{P}^{(1)}(\hat{r}_\sigma) \times \hat{r}_\sigma) \times \hat{r}_\sigma] \end{aligned} \quad (2.38)$$

$$\hat{E}^{(1)}(\vec{R}) = \frac{Z_C I^{(1)}(\vec{R}^{(1)})}{2 \vec{D}_1 \times \vec{D}_2} \sum_{k=-\infty}^{\infty} \sum_{n=-\infty}^{\infty} \frac{e^{-j\beta(\vec{R}-\vec{R}^{(1)}) \cdot \hat{r}_{-\sigma}}}{r_3} \cdot$$

$$\frac{e^{j\beta(\hat{r}_{-\sigma} \cdot \vec{D}_e - s_e)}}{1 - e^{j\beta(\hat{r}_{-\sigma} \cdot \vec{D}_e - s_e)}} [(\hat{P}^{(1)}(\hat{r}_{-\sigma}) \times \hat{r}_{-\sigma}) \times \hat{r}_{-\sigma}]$$
(2.39)

$$\hat{E}_0^{(1)}(\vec{R}) = \frac{Z_C I^{(1)}(\vec{R}^{(1)})}{2 \vec{D}_1 \times \vec{D}_2} \sum_{k=-\infty}^{\infty} \sum_{n=-\infty}^{\infty} \frac{e^{-j\beta(\vec{R}-\vec{R}^{(1)}) \cdot \hat{r}_{\pm}}}{r_3}$$

$$[(\hat{P}^{(1)}(\hat{r}_{\pm}) \times \hat{r}_{\pm}) \times \hat{r}_{\pm}]$$
(2.40)

with

$$\hat{r}_{\pm\sigma} = r_1 \vec{b}^1 + r_2 \vec{b}^2 \pm \sigma r_3 \vec{b}^3$$
(2.41)

Equations (2.23), (2.13), (2.5) - (2.8) are used to find  $r_1, r_2, \vec{b}$ .  
 Notice that  $\hat{E}_0^{(1)}(\vec{R})$  does not depend on  $\vec{D}_e$ .

### C. IMPEDANCE EQUATIONS FOR WIRE ANTENNAS

Place another antenna element with transmitting current distribution  $\overset{(2)}{I}(\overset{+}{R})$  and terminal point  $\overset{+(2)}{R}$  in the region of the volume array. The induced voltage in antenna (2) due to a unit current in antenna array (1) will be the mutual impedance given by

$$\begin{aligned} Z_{\text{volume}}^{2,1}(\overset{+}{D}_1, \overset{+}{D}_2 | \overset{+}{D}_e) &= Z_+^{2,1}(\overset{+}{D}_1, \overset{+}{D}_2 | \overset{+}{D}_e) + Z_0^{2,1}(\overset{+}{D}_1, \overset{+}{D}_2) \\ &\quad + Z_-^{2,1}(\overset{+}{D}_1, \overset{+}{D}_2 | \overset{+}{D}_e) \end{aligned} \quad (2.42)$$

and is obtained by combining Equations (1.1) - (1.2) with Equations (2.37) - (2.40). When  $\overset{(2)}{I}(\overset{+}{R}) = \overset{(1)}{I}(\overset{+}{R})$  and  $\overset{+(2)}{R} = \overset{+(1)}{R}$ , Equation (2.42) yields the self impedance of antenna (1).

Consider first the term due to the  $\ell=0$  plane,  $Z_0^{2,1}(\overset{+}{D}_1, \overset{+}{D}_2)$ . If  $\overset{+}{D}_1$  and  $\overset{+}{D}_2$  are the initial lattice vectors of the nonplanar array, then calculation of  $Z_0^{2,1}(\overset{+}{D}_1, \overset{+}{D}_2)$  leads to iterated integrals which we are trying to avoid. In order to find the nonplanar impedance, we need only calculate the impedance once for the element in some two-dimensional lattice in which it is totally planar. We will assume for this calculation of  $Z_0^{2,1}(\overset{+}{D}_1, \overset{+}{D}_2)$  that  $\overset{+}{D}_1$  and  $\overset{+}{D}_2$  fulfills this condition. In Chapter III, we will use the  $Z_+^{2,1}$  and  $Z_-^{2,1}$  terms to transform the impedance  $Z_0^{2,1}(\overset{+}{D}_1, \overset{+}{D}_2)$  from the planar lattice to the original nonplanar lattice.

If both antenna elements lie completely within the plane of the array, then the self/mutual impedance  $Z_0^{2,1}(\overset{+}{D}_1, \overset{+}{D}_2)$  is evaluated using the

standard method developed by Munk [7]. In this procedure, the induced voltage is found by integrating the field from antenna array (1) due to a filamentary current distribution at  $\hat{R}^{(1)}$  over the filamentary transmitting current distribution of antenna (2) at  $\hat{R}^{(2)} + a^{(2)}\hat{b}^3$ . This point is one wire radius  $a^{(2)}$  of antenna (2) above the plane of the array in the evanescent direction  $\hat{b}^3$ . This method is an approximation of Equation (1.1) which has been shown to produce excellent results by Munk et. al.

For a linear antenna in the direction  $\hat{p}$ , Appendix B shows how the filamentary pattern factor  $\hat{p}^{(1)}(\hat{r})$  is related to the vector pattern function  $\hat{p}^{(1)}(\hat{r})$  by,

$$\hat{p}^{(1)}(\hat{r}) = \hat{p} J_0(\beta a^{(1)} \sqrt{1 - (\hat{r} \cdot \hat{p}^{(1)})^2}) p^{(1)}(\hat{r}) \quad (2.43)$$

where

$$p^{(1)}(\hat{r}) = \frac{1}{I^{(1)}(\hat{R}^{(1)})} \int_{\text{element}} I^{(1)}(\ell) e^{j\beta\ell(\hat{r} \cdot \hat{p}^{(1)})} d\ell. \quad (2.44)$$

$J_0(x)$  is the Bessel function of order zero and  $a^{(1)}$  is the radius of antenna (1). Equation (2.43) is derived by averaging  $\hat{p}p^{(1)}(\hat{r})$  around a circle orthogonal to  $\hat{p}$  and of radius  $a^{(1)}$ .

Replacing  $\hat{p}^{(1)}(\hat{r})$  with  $\hat{p}^{(1)}p^{(1)}(\hat{r})$  in Equation (2.40) and performing the integration gives

$$Z_0^{2,1}(\vec{D}_1, \vec{D}_2) = \frac{-Z_C}{2\|\vec{D}_1 \times \vec{D}_2\|} \sum_{k=-\infty}^{\infty} \sum_{n=-\infty}^{\infty} \frac{e^{-j\beta(\vec{R}^{(2)} + \vec{a}^{(2)} + \vec{b}^{(2)} - \vec{R}^{(1)}) \cdot \hat{r}_{\pm}}}{r_3} [(\hat{p}^{(1)} \times \hat{r}_{\pm}) \times \hat{r}_{\pm}] \cdot \hat{p}^{(2)} p^{(1)}(\hat{r}_{\pm}) p^{(2)} t(\hat{r}_{\pm})$$
(2.45)

with the filamentary transmitting pattern factor defined by

$$p^{(2)} t(\hat{r}) = \frac{1}{I^{(2)} t(\vec{R}^{(2)})} \int_{\text{element}} I^{(2)} t(\vec{\ell}) e^{-j\beta \ell \cdot (\hat{r} \cdot \hat{p}^{(2)})} d\ell. \quad (2.46)$$

Equation (2.45) is also valid if antenna (2) is outside Region 2 of antenna (1).

The terms  $Z_+^{2,1}(\vec{D}_1, \vec{D}_2 | \vec{D}_e)$  and  $Z_-^{2,1}(\vec{D}_1, \vec{D}_2 | \vec{D}_e)$  are a straightforward application of Equation (1.1) and Equations (2.38) - (2.39) and are valid for any element orientation within the region of validity indicated in Figure 2.3,

$$Z_+^{2,1} = \frac{-Z_C}{2\|\vec{D}_1 \times \vec{D}_2\|} \sum_{k=-\infty}^{\infty} \sum_{n=-\infty}^{\infty} \frac{e^{-j\beta(\vec{R}^{(2)} - \vec{R}^{(1)}) \cdot \hat{r}_{\sigma}}}{r_3} \frac{e^{-j\beta(\vec{r}_{\sigma} \cdot \vec{D}_e - s_e)}}{1 - e^{-j\beta(\vec{r}_{\sigma} \cdot \vec{D}_e - s_e)}} [(\hat{p}^{(1)}(\hat{r}_{\sigma}) \times \hat{r}_{\sigma}) \times \hat{r}_{\sigma}] \cdot \hat{p}^{(2)} t(\hat{r}_{\sigma})$$
(2.47)

$$Z_{\infty}^{2,1} = \frac{-Z_C}{2iD_1 \times D_2} \sum_{k=-\infty}^{\infty} \sum_{n=-\infty}^{\infty} \frac{e^{-j\beta(\hat{R}^{(2)} - \hat{R}^{(1)}) \cdot \hat{r}_{-\sigma}}}{r_3}$$

$$\frac{e^{j\beta(\hat{r}_{-\sigma} \cdot \hat{D}_e - s_e)}}{1 - e^{j\beta(\hat{r}_{-\sigma} \cdot \hat{D}_e - s_e)}} [(\hat{p}^{(1)}(\hat{r}_{-\sigma}) \times \hat{r}_{-\sigma}) \times \hat{r}_{-\sigma}] \cdot \hat{p}^{(2)t}(\hat{r}_{-\sigma})$$
(2.48)

where

$$\hat{p}^{(2)t}(\hat{r}) = \frac{1}{I^{(2)t}(\hat{R}^{(2)})} \int_{\text{element}} \hat{I}^{(2)t}(\hat{R}') e^{-j\beta \hat{R}' \cdot \hat{r}} d\hat{R}' \quad (2.49)$$

is the vector transmitting pattern function. It is similarly related to the filamentary transmitting pattern factor by

$$\hat{p}^{(2)t} = \hat{p}^{(2)} J_0 (\beta a^{(2)} \sqrt{1 - (\hat{r} \cdot \hat{p}^{(2)})^2}) p^{(2)t}(\hat{r}) . \quad (2.50)$$

Equations (2.43) and (2.50) may be easily extended to a piecewise combination of linear antenna sections.

#### D. THE EXCITATION VECTOR $\vec{s}$

When using the volume impedance Equations (2.47) - (2.48) to calculate the nonplanar self/mutual impedance of an array defined by direct lattice vectors  $\vec{D}_1$  and  $\vec{D}_2$ , the vector  $\vec{D}_e$  is a dummy vector which is usually chosen in the same plane as the antenna elements but is otherwise arbitrary. Likewise,  $s_1 = \vec{s} \cdot \vec{D}_1$  and  $s_2 = \vec{s} \cdot \vec{D}_2$  are fixed by the scan angle (e.g., Equation (2.18)) while  $s_e = \vec{s} \cdot \vec{D}_e$  is arbitrary. A logical choice for  $s_e$  would appear to be the one which makes  $\vec{s}$  a unit vector  $\hat{s}$ . But when  $\hat{s} = \hat{s}$ , either  $(\hat{r}_\sigma - \hat{s}) = 0$  or  $(\hat{r}_{-\sigma} - \hat{s}) = 0$  in the  $k=0, n=0$  term in Equations (2.47) - (2.48). This produces a pole in the  $Z_{\text{volume}}^{2,1}$  impedance which is unacceptable for our purposes. A safe choice is  $s_e = 0$ .

The fact that the equations blow up when  $\vec{s}$  is a unit vector may at first be disturbing but is actually related to the nature of a space filled by a volume array. The presence of the array changes the effective constitutive parameters of the space in a manner similar to a dielectric. The application of this principle to metallic delay lenses was first demonstrated by Koch [8].

The effective vector wave number  $\vec{k}_0$  of this artificial medium at a given frequency  $\omega_0$  is determined by the condition of a zero tangential electric field along the antenna elements without an external voltage excitation. This corresponds to an eigenfunction of the periodic structure and is equivalent to the requirement

$$Z_{\text{volume}}(\vec{s}_0) = 0 , \quad (2.51)$$

$$\vec{k}_0 = \beta \vec{s}_0 . \quad (2.52)$$

With these conditions fulfilled, the total self induced voltage is zero with a nonzero current distribution given by Equations (2.24) and (2.52),

$$\vec{I}_{qml}(R) = \vec{I}_{000}(R-R_{qml}) e^{-j\vec{R}_{qml} \cdot \vec{k}_0} . \quad (2.53)$$

This current is a plane wave propagating through the periodic structure with phase velocity  $\omega_0/|\vec{k}_0|$  and group velocity  $d\omega_0/d|\vec{k}_0|$ . We would expect the presence of the array to change the effective parameters of the medium so that  $|\vec{k}_0| \neq \beta$  in Equation (2.52). In this case,  $\vec{s}_0$  is not a unit vector.

Without the array, a plane wave would propagate through the medium at frequency  $\omega_0$  with  $\vec{s} = \hat{s}$  a unit vector. We have seen before how the self impedance goes to infinity when the volume array in the medium is excited in this manner. This gives the interesting result that a volume array in a medium with wave number  $\beta$  can not support a plane wave with wave number  $|\vec{k}_0| = \beta$ . The exception to this rule occurs when there is a null in the pattern function in the direction of propagation  $\vec{k}_0$ .

The periodic volume array as an artificial dielectric is not relevant to the main objective of this report. The preceding discussion is only meant to illustrate the nature of the vector  $\vec{s}$  and why the arbitrary component  $s_e = \vec{s} \cdot \vec{D}_e$  may be chosen to be almost any value except the one which makes  $\vec{s} = \hat{s}$  a unit vector. As mentioned before,  $s_e = 0$  is usually a safe choice.

## CHAPTER III

### THE NONPLANAR IMPEDANCE

#### A. GENERAL CONSIDERATIONS

A planar array in a homogeneous space is uniquely defined by its reference position  $\overset{+}{R}^{(1)}$ , the orientation and dimensions of the elements relative to  $\overset{+}{R}^{(1)}$ , and the lattice vectors  $\overset{+}{D}_1$  and  $\overset{+}{D}_2$ . When the elements are tipped out of the plane of the array, the calculation of the self/mutual impedances becomes very difficult because of the iterated integration. However, the use of volume impedances allows one to transform the problem from the  $\overset{+}{D}_1, \overset{+}{D}_2$  lattice to the  $\overset{+}{D}_3, \overset{+}{D}_4$  lattice where impedances are more easily evaluated. In doing this transformation, the element's position  $\overset{+}{R}^{(1)}$  and orientation remain the same; only the lattice vectors change.

For a volume distribution of elements defined by the direct lattice vectors  $\overset{+}{D}_1, \overset{+}{D}_2, \overset{+}{D}_3$ , the self/mutual impedance has been derived in Chapter II as

$$z_{\text{volume}}^{2,1} = z_0^{2,1}(\overset{+}{D}_1, \overset{+}{D}_2) + z_+^{2,1}(\overset{+}{D}_1, \overset{+}{D}_2 | \overset{+}{D}_3) + z_-^{2,1}(\overset{+}{D}_1, \overset{+}{D}_2 | \overset{+}{D}_3) .$$

(3.1)

Or by symmetry,

$$Z_{\text{volume}}^{2,1} = Z^{2,1}(\vec{D}_2, \vec{D}_3) + Z^{2,1}_+(\vec{D}_2, \vec{D}_3 | \vec{D}_1) + Z^{2,1}_-(\vec{D}_2, \vec{D}_3 | \vec{D}_1). \quad (3.2)$$

The evanescent direction  $\vec{D}_e$  has been chosen as  $\vec{D}_3$  in the first case and  $\vec{D}_1$  in the second case. Combining Equations (3.1) - (3.2) gives

$$Z_0^{2,1}(\vec{D}_1, \vec{D}_2) = Z_0^{2,1}(\vec{D}_2, \vec{D}_3) + Z_\Delta^{2,1}(\vec{D}_2 | \vec{D}_1 + \vec{D}_3) \quad (3.3)$$

with

$$\begin{aligned} Z_\Delta^{2,1}(\vec{D}_2 | \vec{D}_1 + \vec{D}_3) &= Z^{2,1}_+(\vec{D}_2, \vec{D}_3 | \vec{D}_1) + Z^{2,1}_-(\vec{D}_2, \vec{D}_3 | \vec{D}_1) \\ &- Z^{2,1}_+(\vec{D}_1, \vec{D}_2 | \vec{D}_3) - Z^{2,1}_-(\vec{D}_1, \vec{D}_2 | \vec{D}_3). \end{aligned} \quad (3.4)$$

Equation (3.3) is the basic formula for calculating nonplanar impedances. As long as the intermediate step of forming a volume array is valid, the impedance terms in Equation (3.4) are always calculable and have a strong exponential convergence.

If the array is still nonplanar in the  $\vec{D}_2, \vec{D}_3$  lattice but planar in the  $\vec{D}_3, \vec{D}_4$  lattice, another transform may be possible.

$$Z_0^{2,1}(\vec{D}_2, \vec{D}_3) = Z_0^{2,1}(\vec{D}_3, \vec{D}_4) + Z_\Delta^{2,1}(\vec{D}_3 | \vec{D}_2 + \vec{D}_4). \quad (3.5)$$

Combining with Equation (3.3) gives

$$z_0^{2,1}(\vec{D}_1, \vec{D}_2) = z_0^{2,1}(\vec{D}_3, \vec{D}_4) + z_{\Delta}^{2,1}(\vec{D}_2 | \vec{D}_1 + \vec{D}_3) + z_{\Delta}^{2,1}(\vec{D}_3 | \vec{D}_2 + \vec{D}_4) . \quad (3.6)$$

The same vector pattern functions  $\hat{p}^{(1)}(\hat{r})$ ,  $\hat{p}^{(2)t}(\hat{r})$  and filamentary pattern factors  $p^{(1)}(\hat{r})$ ,  $p^{(2)t}(\hat{r})$  are used throughout these transforms since the elements maintain the same orientation.

## B. DIPOLE ARRAY

Consider an array of linear dipole antennas with arbitrary orientation  $\hat{p}$  in a rectangular grid with interelement spacings  $D_x$  and  $D_z$  as shown in Figures 1.1 and 3.1. Equation (3.3) will be used to find the self impedance. For this geometry

$$\begin{aligned}\vec{D}_1 &= \hat{x} D_x \\ \vec{D}_2 &= \hat{z} D_z .\end{aligned}\quad (3.7)$$

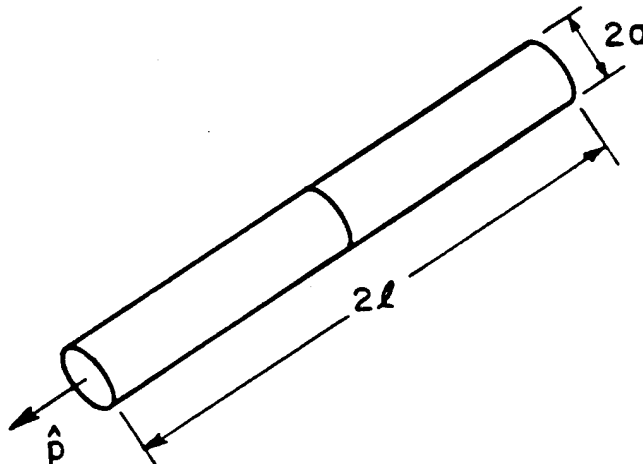


Figure 3.1. Single dipole used in the example.

We will assume a linear phase difference between elements characterized by a plane wave  $\hat{E}_0 e^{-j\beta s \cdot \hat{R}}$  excitation;

$$\begin{aligned}s_x &= \hat{s} \cdot \hat{x} \\ s_z &= \hat{s} \cdot \hat{z}\end{aligned}\quad (3.8)$$

and therefore,

$$\begin{aligned}s_1 &= s_x D_x \\ s_2 &= s_z D_z .\end{aligned}\quad (3.9)$$

The antenna elements have a half length  $\ell$  and radius  $a$ . We will choose,

$$\begin{aligned}\hat{D}_3 &= 2.5 \ell \hat{p} \\ s_3 &= 0 .\end{aligned}\quad (3.10)$$

This choice insures a valid volume array and insures the dipole array will be totally planar in the  $\hat{D}_2, \hat{D}_3$  lattice ( $\hat{z} \cdot \hat{p}$  plane). A larger  $\|\hat{D}_3\|$  means a faster converging  $Z_{\pm}(\hat{D}_1, \hat{D}_2 | \hat{D}_3)$  term but a slower converging  $Z_0(\hat{D}_2, \hat{D}_3)$  term. Equation (2.45) is now used to calculate the planar  $Z_0(\hat{D}_2, \hat{D}_3)$  impedance and Equations (2.47), (2.48) and (3.4) are used to find the difference  $Z_{\Delta}(\hat{D}_2 | \hat{D}_1 + \hat{D}_3)$  impedance. Adding gives the self impedance of the nonplanar dipole array. Figure 3.3 shows the scan impedance for the case,

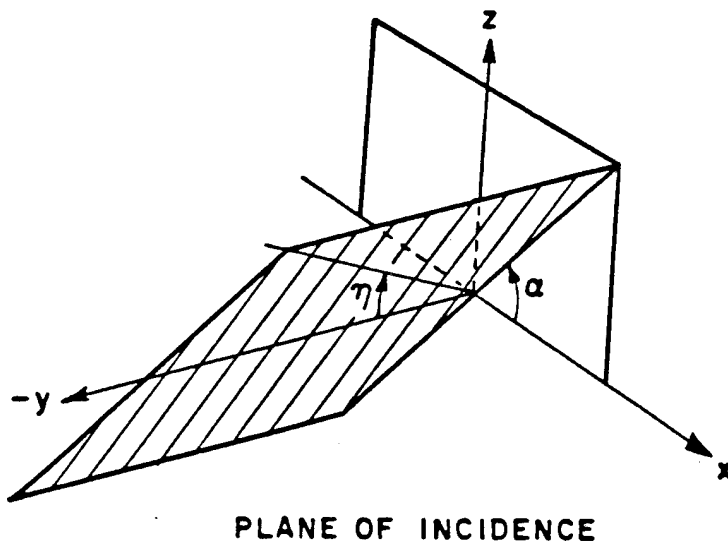


Figure 3.2. Incident angle parameters  $\alpha$  and  $\eta$ .

$$D_x = D_z = 1 \text{ cm}$$

$$\hat{p} = -y$$

$$\ell = .68 \text{ cm}$$

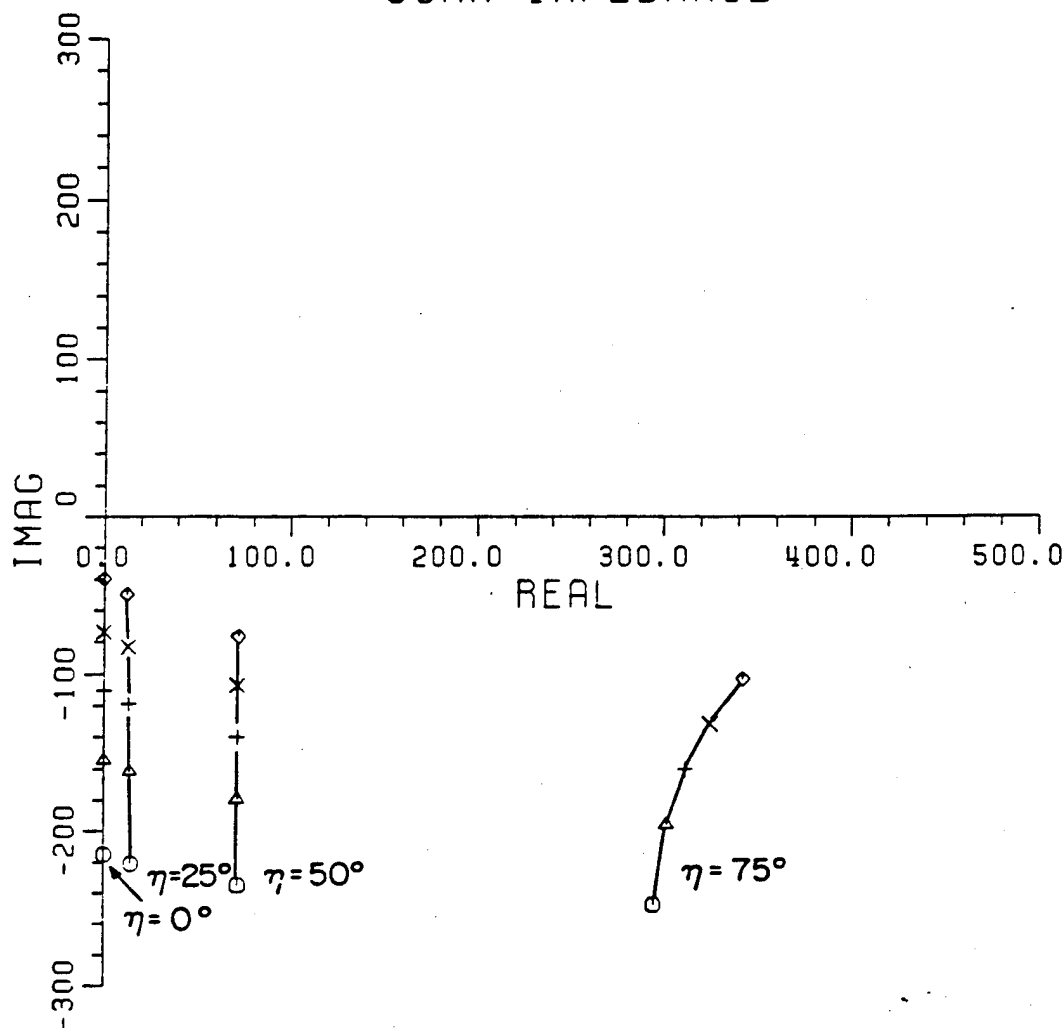
$$a = .05 \text{ cm}$$

$$\epsilon = 2.17 .$$

The incident angle parameters  $\alpha$  and  $\eta$  are illustrated in Figure 3.2.

As another simple example, the mutual impedance is calculated for two  $\hat{y}$  directed dipole arrays having the same parameters as the first example as a function of their separation in the  $\hat{z}$ - $\hat{y}$  plane. The positions of the two reference elements are

## SCAN IMPEDANCE



ALPHA = 0.00	
F (GHZ) = 4.00	○
F (GHZ) = 5.00	△
F (GHZ) = 6.00	+
F (GHZ) = 7.00	×
F (GHZ) = 8.00	◊

Figure 3.3. Scan impedance for an array of  $\hat{y}$  directed dipoles for various angles of incidence and frequencies.

$$\vec{R}^{(1)} = \text{origin}$$

$$\vec{R}^{(2)} = 0_y \hat{y} + 0_z \hat{z} \quad (3.11)$$

where the offsets  $0_y$  and  $0_z$  are measured in cm. Figure 3.4 shows the geometry of the problem and figures 3.5 through 3.9 show the scan impedance for various offsets and angles of incidence with  $\alpha=90^\circ$ . In this case,  $\vec{D}_3$  was chosen as

$$\vec{D}_3 = -4\ell \hat{y} \quad (3.12)$$

which was sufficient for the examples treated.

### C. LOOP ARRAY

A common method for constructing nonplanar phased arrays is to etch one row of elements on printed circuit boards as in Figure 3.10 and then stack the boards to form the  $\vec{D}_1, \vec{D}_2$  planar lattice shown in Figure 3.11. By choosing  $\vec{D}_3$  in the plane of the pc boards, the  $\vec{D}_1, \vec{D}_3$  plane may be used to calculate  $Z_0^{2,1}(\vec{D}_1, \vec{D}_3)$  for all self and mutual impedances between antenna elements. As before, this planar impedance is readily transformed into  $Z_0^{2,1}(\vec{D}_1, \vec{D}_2)$  for the nonplanar lattice. This is perhaps the most useful application of this method because of the ease with which complex current distributions and modes may be intermixed.

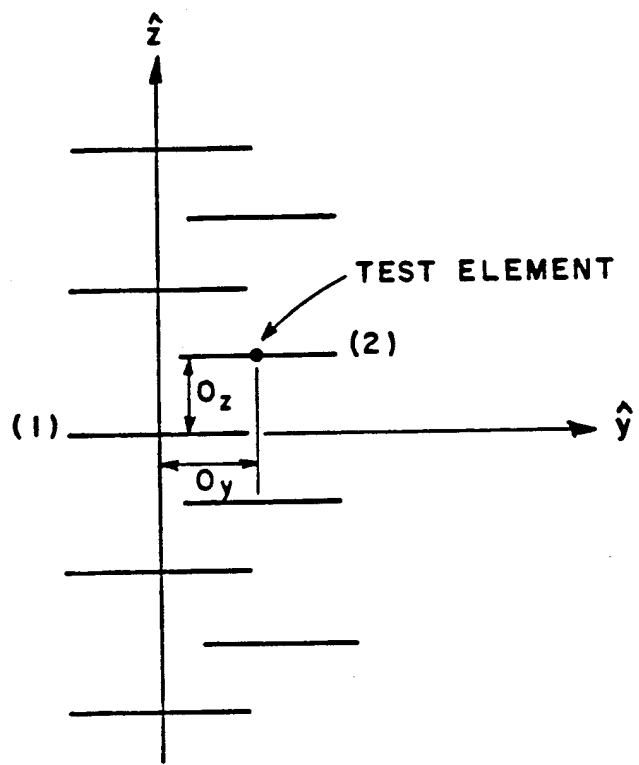
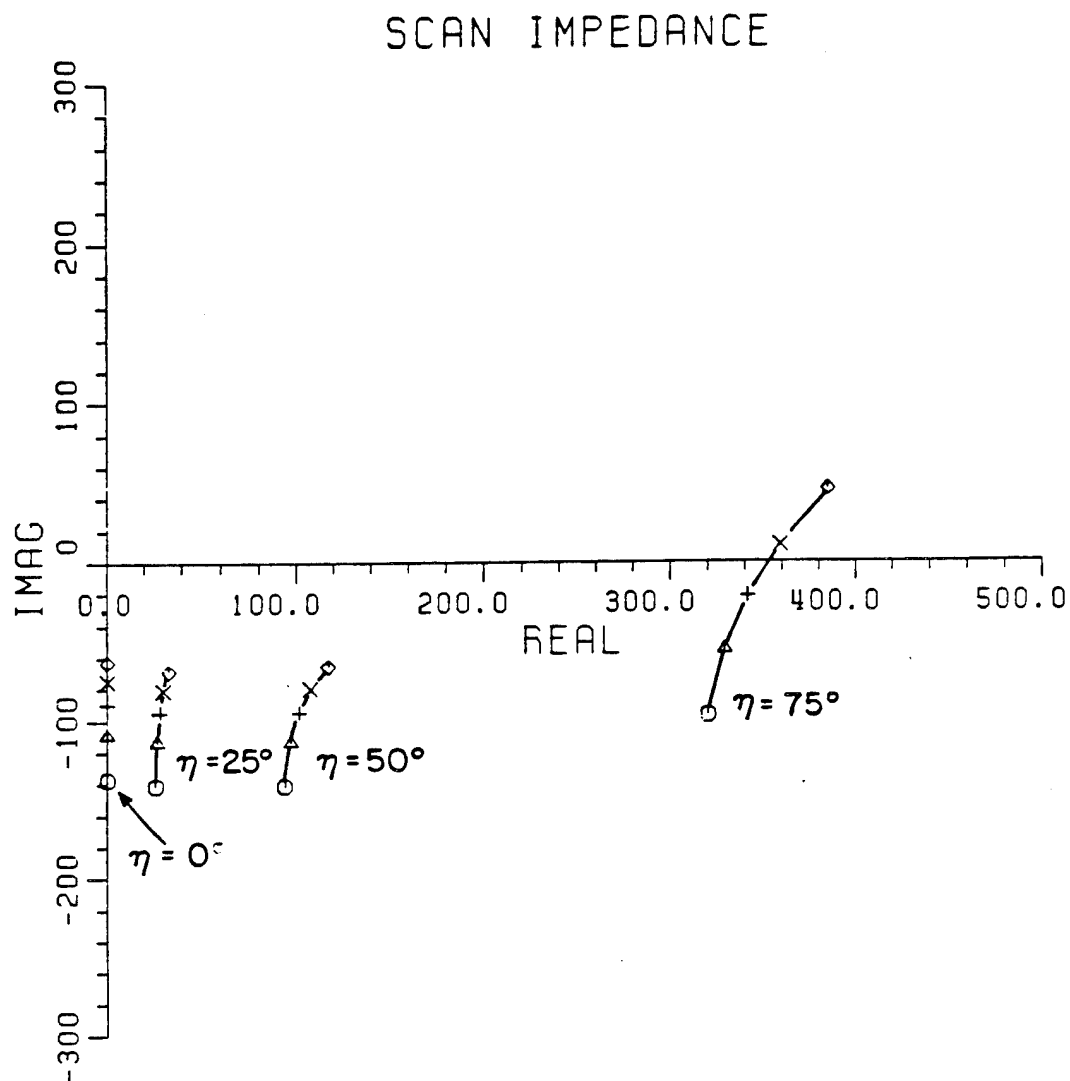


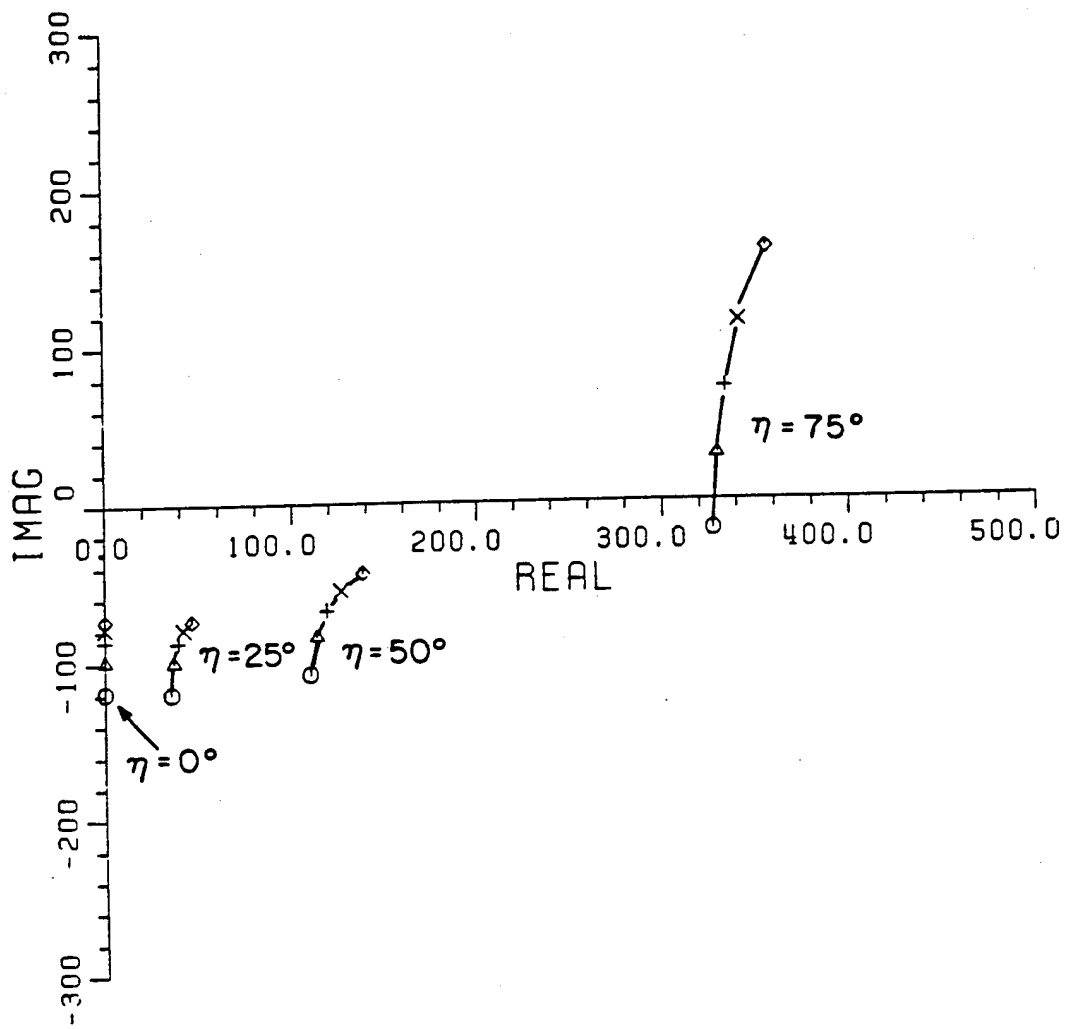
Figure 3.4. Example of mutual impedance calculations.



ALPHA = 90.00	0Z = 0.20
F (GHZ) = 4.00	0Y = 0.00
F (GHZ) = 5.00	△
F (GHZ) = 6.00	+
F (GHZ) = 7.00	×
F (GHZ) = 8.00	◊

Figure 3.5. Mutual impedance between  $\hat{y}$  directed dipole arrays with separation  $0_y=0.0$ ,  $0_z=0.2$ .

## SCAN IMPEDANCE



ALPHA = 90.00	0Z = 0.35
F (GHZ) = 4.00	0Y = 0.00
F (GHZ) = 5.00	○
F (GHZ) = 6.00	▲
F (GHZ) = 7.00	+
F (GHZ) = 8.00	×

Figure 3.6. Mutual impedance between  $\hat{y}$  directed dipole arrays with separation  $0_y = 0.0$ ,  $0_z = 0.35$ .

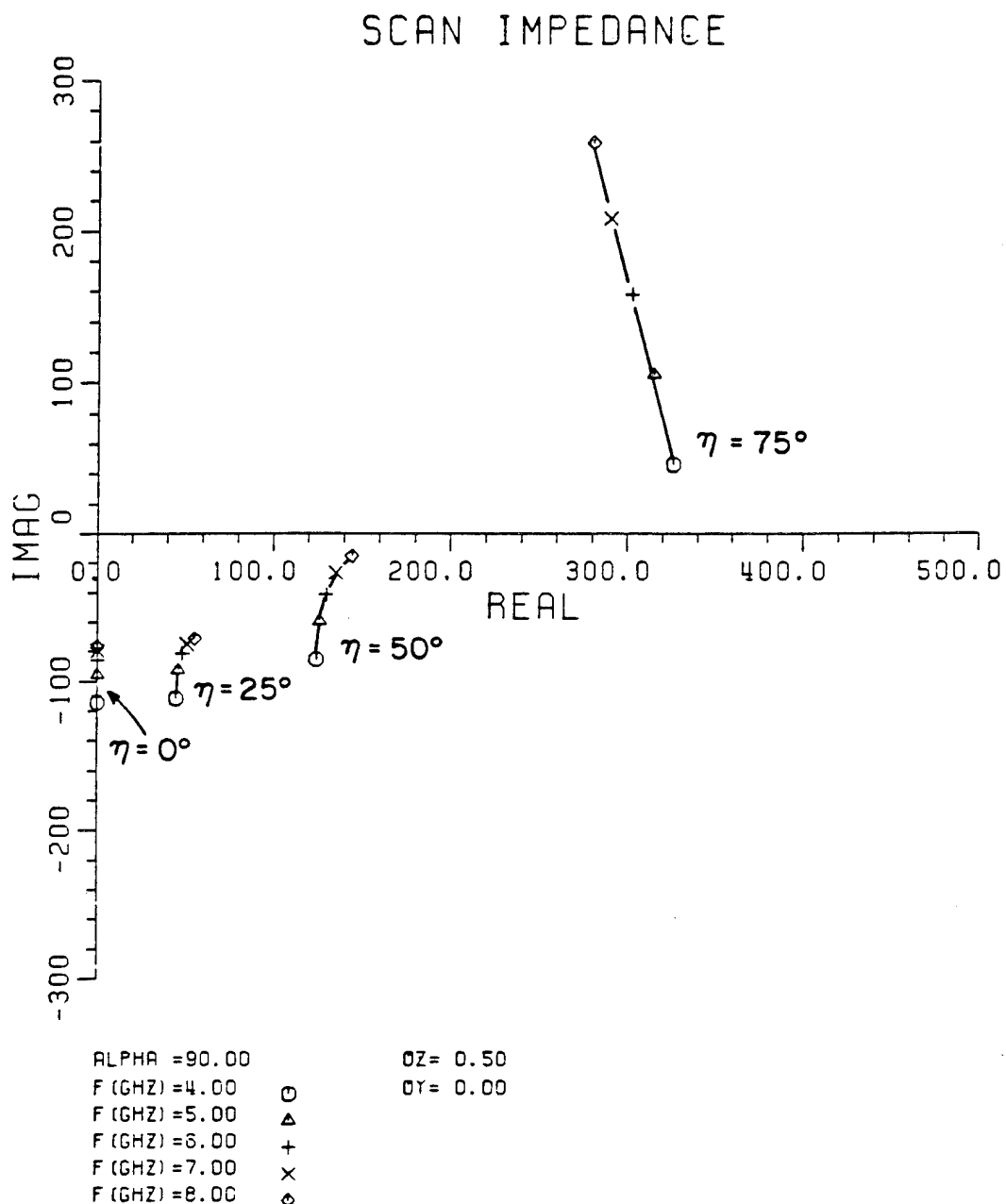


Figure 3.7. Mutual impedance between  $\hat{y}$  directed dipole arrays with separation  $\theta_y = 0.0$ ,  $\theta_z = 0.5$ .

### SCAN IMPEDANCE

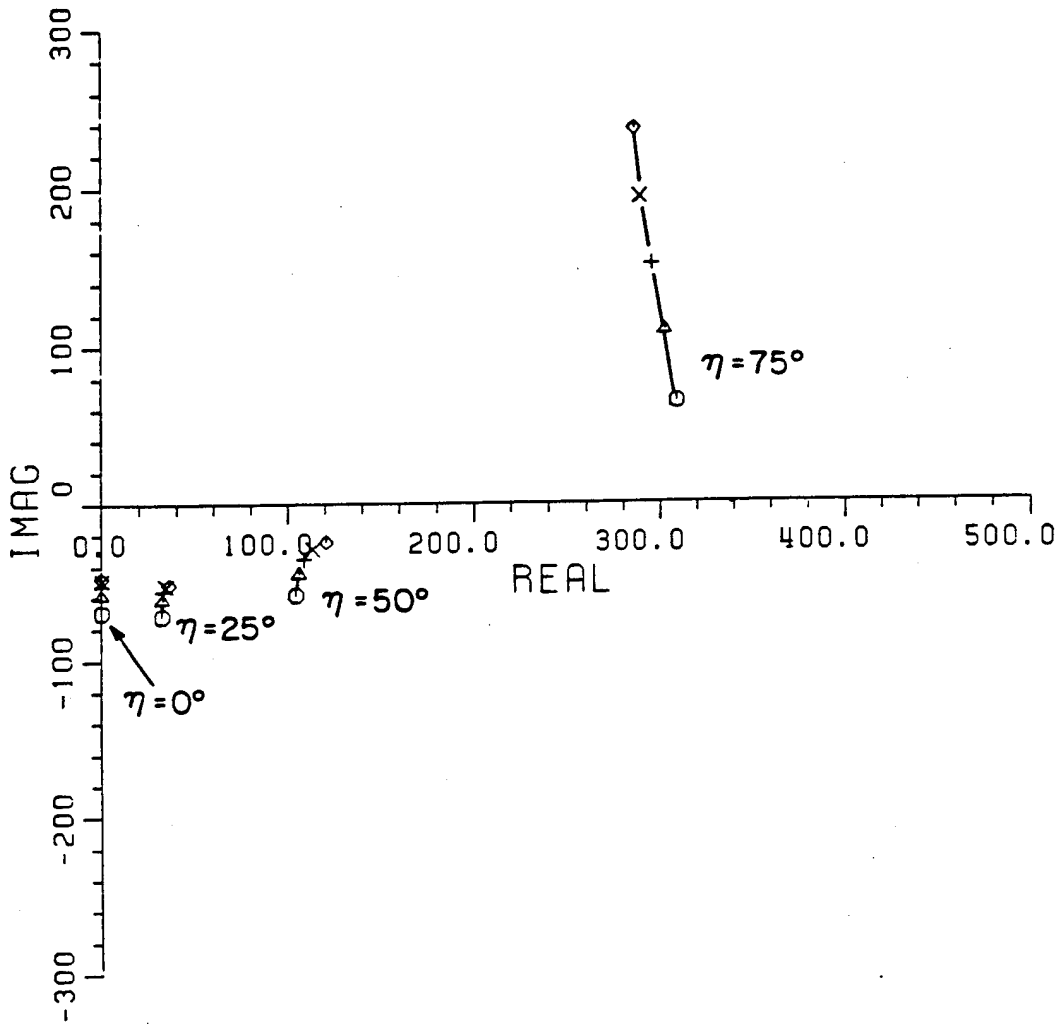


Figure 3.8. Mutual impedance between  $y$  directed dipole arrays with separation  $0_y = -0.5$ ,  $0_z = 0.5$ .

### SCAN IMPEDANCE

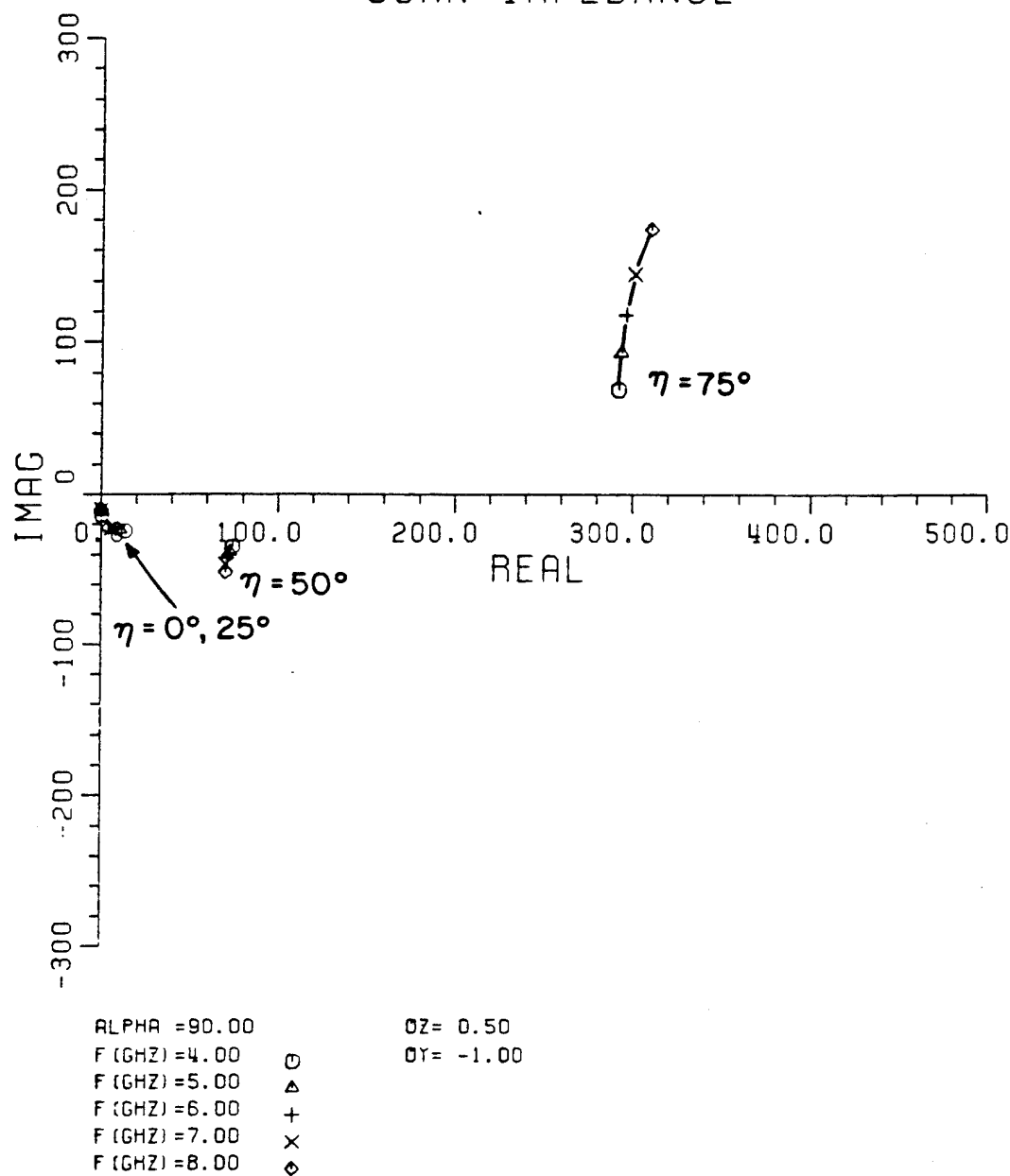


Figure 3.9. Mutual impedance between  $\hat{y}$  directed dipole arrays with separation  $0_y = -1.0$ ,  $0_z = 0.5$ .

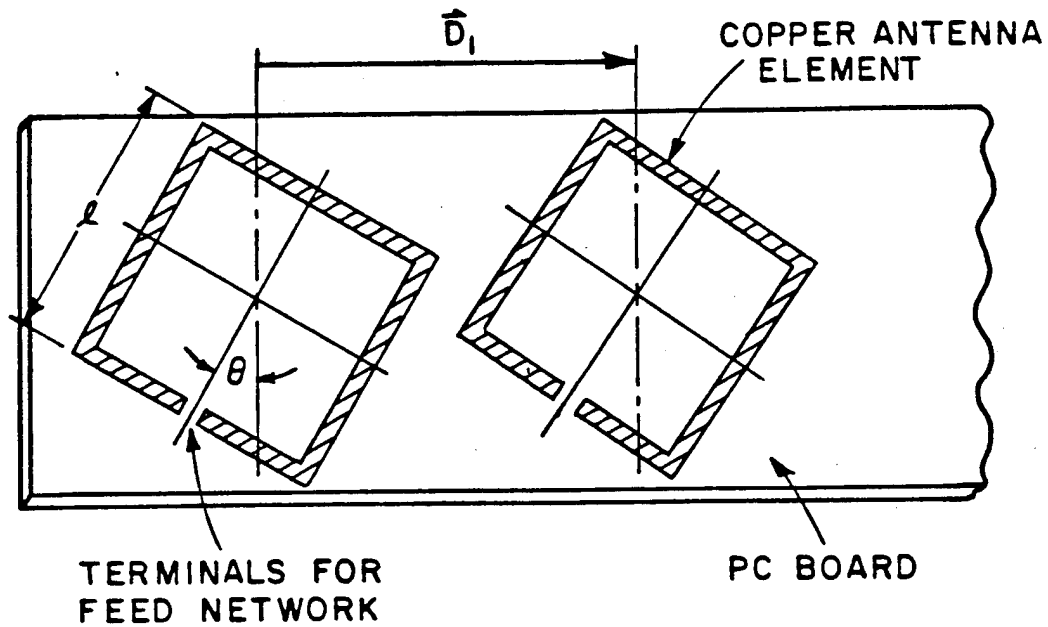


Figure 3.10. Single row of loop antennas etched on a copper clad pc board with interelement spacing  $\vec{D}_1$ . Rotation angle  $\theta$  is used in the example.

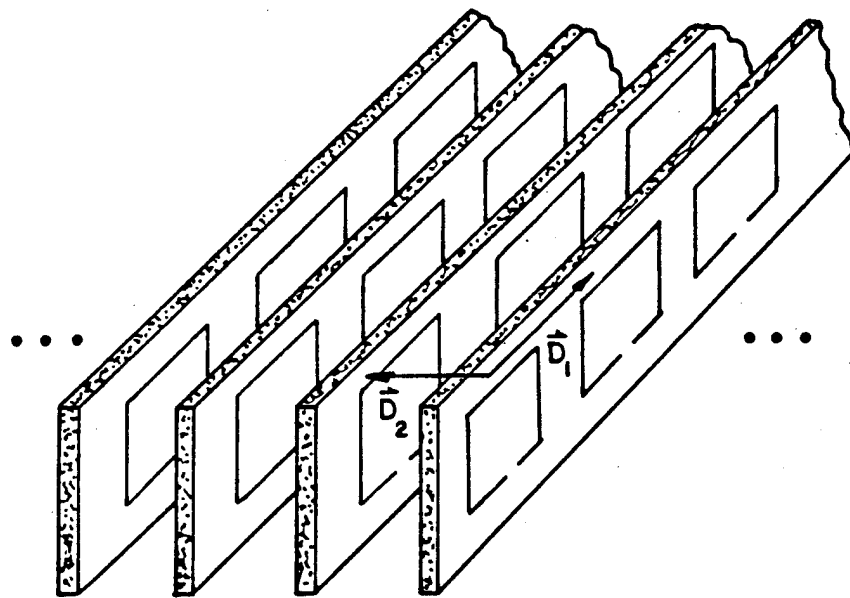


Figure 3.11. Nonplanar array formed by stacking pc boards.

We will consider as an example an array of square loop antennas arranged in a hexagonal lattice in the  $\hat{x}$ - $\hat{z}$  plane. The loops will be rotated in an angle  $\theta$  in the plane of the pc boards as shown in Figure 3.10. The pc boards will be stacked so that they are rotated by an angle  $\phi$  relative to the plane of the array. Figure 3.12 is an edge on view of the pc boards and the plane of the array with  $\vec{D}_1$  pointing into the page. The hexagonal lattice with  $\theta=0$  and  $\phi=0$  is shown in Figure 3.13; only the edge of the loops are visible. By definition,  $\|\vec{D}_1\| = \|\vec{D}_2\|$  and the angel between  $\vec{D}_1$  and  $\vec{D}_2$  is  $\pi/3$  for this lattice. An examination of the reciprocal lattice would show that it is also hexagonal.

We will assume the same symmetrical cosine current distribution for transmitting and receiving as used by Kent.

The planar self impedance will be evaluated in the  $(\vec{D}_1, \vec{D}_3)$  plane and then transformed to the  $(\vec{D}_1, \vec{D}_2)$  plane. A convenient choice for  $\vec{D}_3$  is

$$\vec{D}_3 = 2\ell(\sin\phi\hat{x} - \cos\phi\hat{y}) \quad (3.13)$$

and  $s_3$  is chosen to be zero as usual.

Figures 3.14 - 3.17 show the self impedance of this array in a homogeneous  $\epsilon=2.17$  space with the following parameters:

$$\begin{aligned}\|\vec{D}_1\| &= 1.07 \text{ cm} \\ \ell &= .68 \text{ cm} \\ a &= .05 \text{ cm} \\ \epsilon &= 2.17 \text{ cm} \\ \theta &= 0^\circ, 45^\circ \\ \phi &= 0^\circ, 45^\circ.\end{aligned}$$

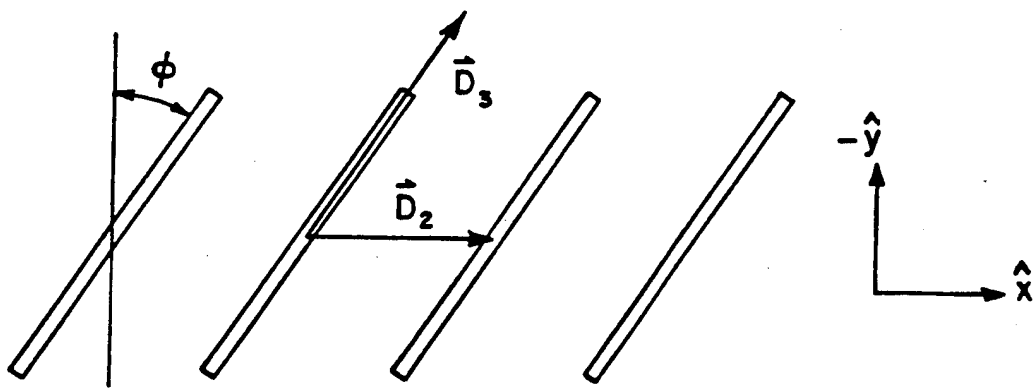


Figure 3.12. Stacked pc boards seen edge on and rotated by the angle  $\phi$ .

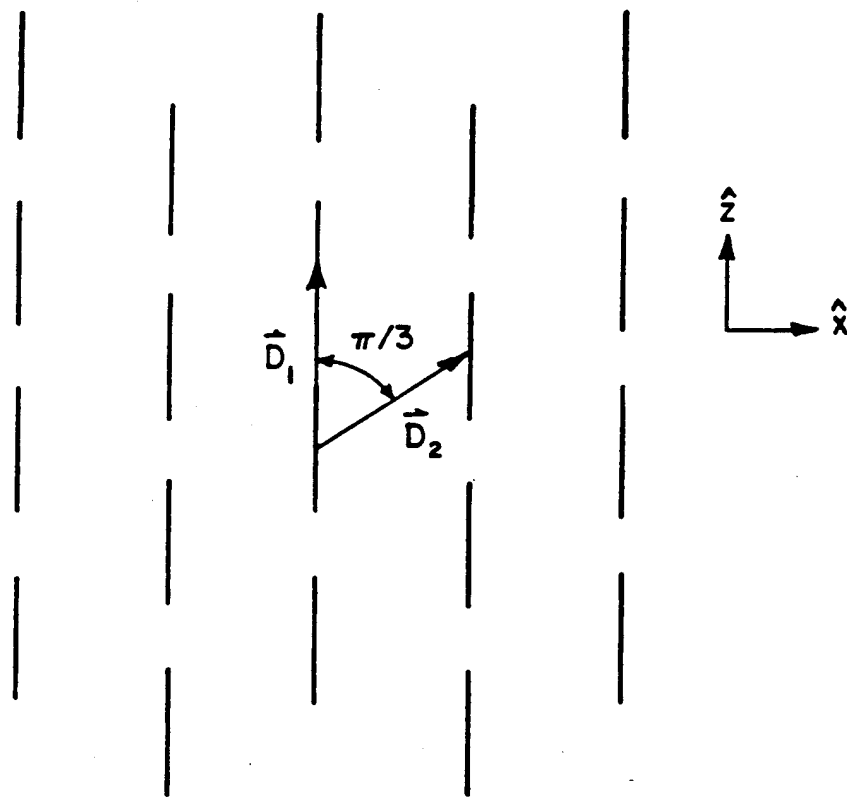


Figure 3.13. With  $\theta=0$  and  $\phi=0$ , only the edge of the loops can be seen looking down onto the hexagonal lattice.

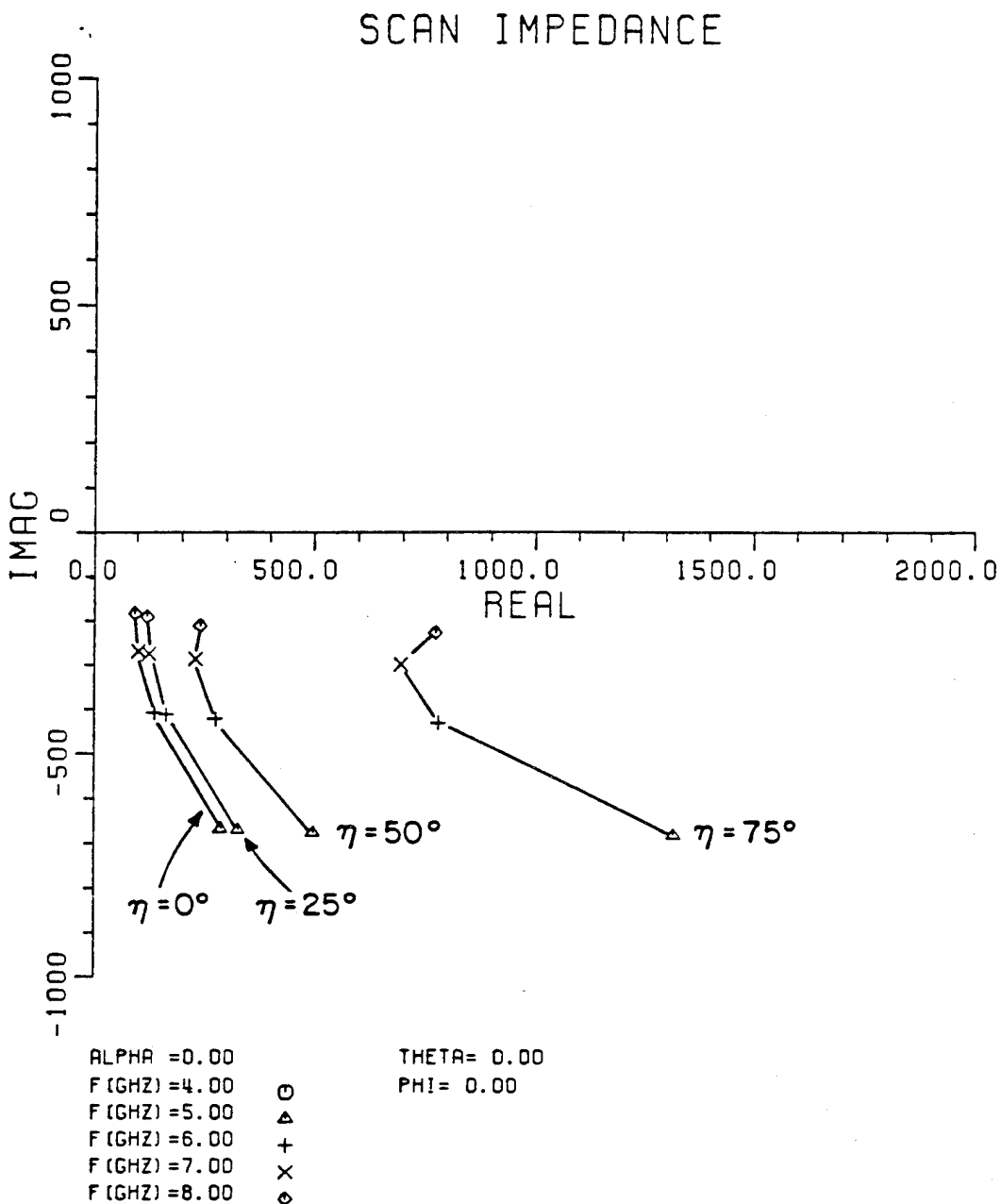


Figure 3.14. Self impedance for a loop array with  $\theta=0^\circ$  and  $\phi=0^\circ$ .

### SCAN IMPEDANCE

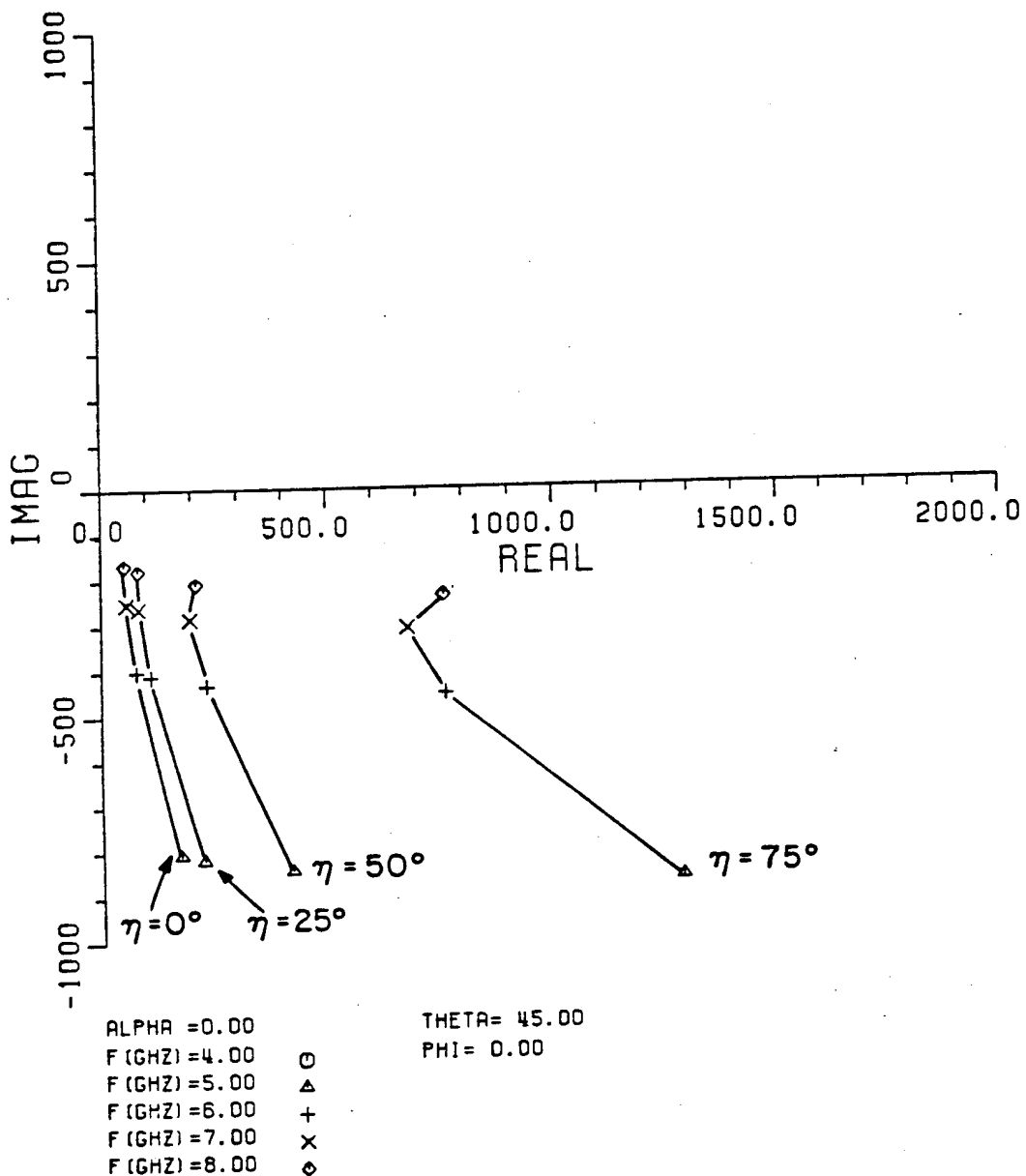


Figure 3.15. Self impedance for a loop array with  $\theta=45^\circ$  and  $\phi=0^\circ$ .

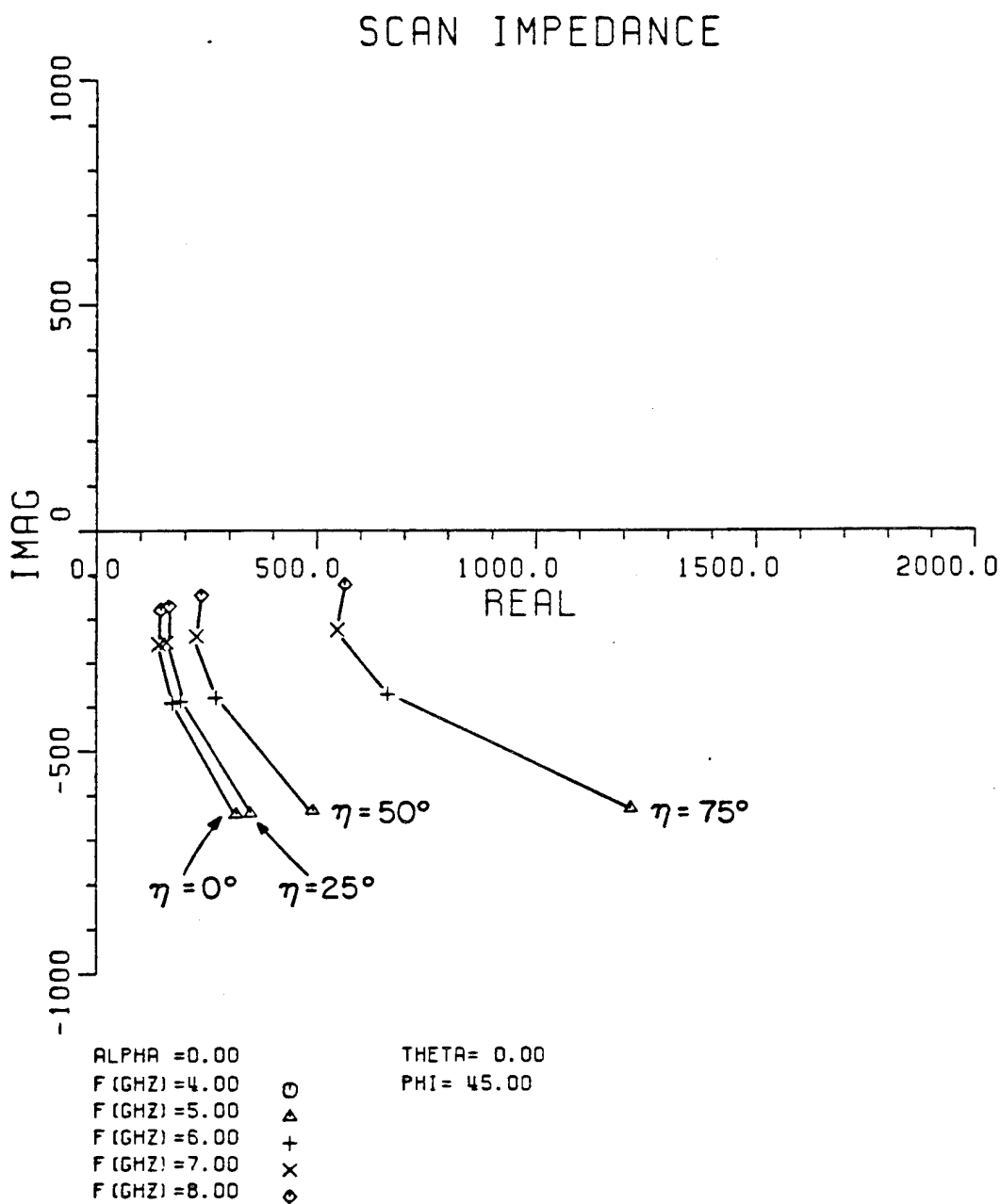


Figure 3.16. Self impedance for a loop array with  $\theta=0^\circ$  and  $\phi=45^\circ$ .

## SCAN IMPEDANCE

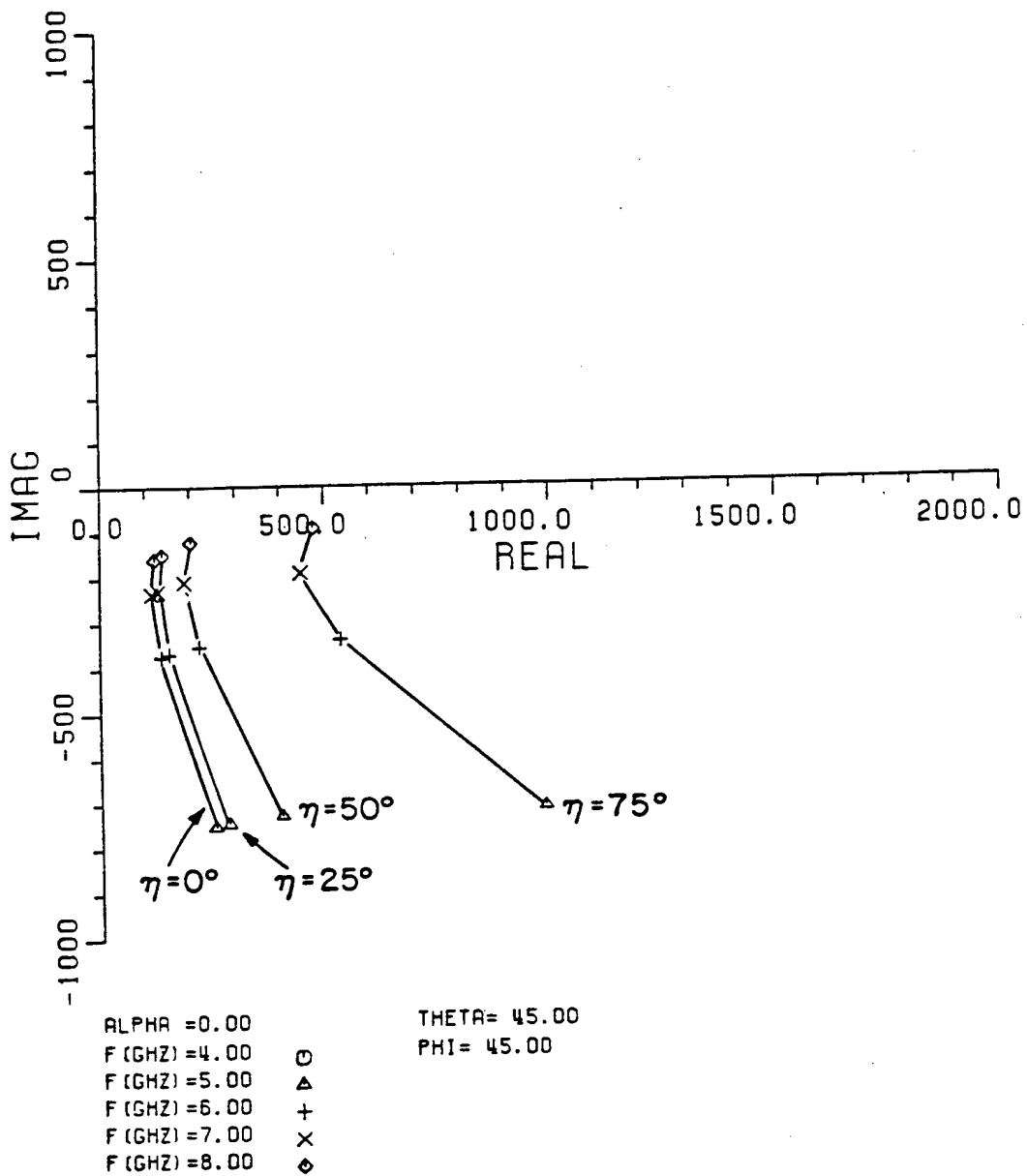


Figure 3.17. Self impedance for a loop array with  $\theta=45^\circ$  and  $\phi=45^\circ$ .

## CHAPTER IV

### CONCLUSION

The method of transforming the impedance between different lattices as presented in the previous chapters can be a very useful tool for analyzing nonplanar arrays. Its value depends heavily on the application. For unusual current distributions with several overlapping modes all confined to the same plane outside the plane of the array, this method would be the only practical approach. However, for elements with a three-dimensional structure, the iterated integral approach may provide the only solution. Either way, the researcher must pay careful attention to the geometry of the problem. Given a choice, the transform method can provide an exponentially converging double summation in all its terms as opposed to the algebraic convergence obtained using iterated integrals.

Only analysis has been considered so far. Equally important for a model is its design potential or the ease with which the equations can be broken down into simpler, more manageable form. Both the transform method because of its dummy lattice vectors and the iterated integral method because of its cumbersome complexity fail miserably. The power of the plane wave expansion comes from the simple cause and effect form which it takes for a totally planar array. Future research in nonplanar arrays should address this issue.

## APPENDIX A

### DERIVATION OF THE FIELDS FROM A PLANAR ARRAY

In this appendix, the field from an infinite planar lattice of current sources will be derived. The geometry is shown in Figure 2.1 with  $\vec{R}^{(1)}$  = origin. The lattice is defined by the two vectors  $\vec{d}_1$  and  $\vec{d}_2$  and the current  $\vec{I}_{qm}(\vec{R})$  associated with the  $q, m^{\text{th}}$  lattice point  $\vec{R}_{qm}$  will be

$$\vec{I}_{qm}(\vec{R}) = \vec{I}_{00}(\vec{R} - \vec{R}_{qm}) e^{-j\beta s \cdot \hat{\vec{R}}_{qm}} \quad (\text{A1})$$

with

$$\vec{R}_{qm} = q\vec{d}_1 + m\vec{d}_2 \quad (\text{A2})$$

upon excitation by a plane wave  $E_0 e^{-j\beta s \cdot \hat{\vec{R}}}$ . Equation (A1) is simply a statement of Floquet's theorem. Alternatively, this current may be impressed on the elements by an external generator.  $\vec{I}_{00}(\vec{R})$  is the current distribution of the  $q=0, m=0$  element relative to the origin.

The total current is

$$\vec{I}(\vec{R}) = \sum_{q=-\infty}^{\infty} \sum_{m=-\infty}^{\infty} \vec{I}_{qm}(\vec{R}) \quad (\text{A3})$$

$$= \sum_{q=-\infty}^{\infty} \sum_{m=-\infty}^{\infty} \vec{I}_{00}(\vec{R} - \vec{R}_{qm}) e^{-j\beta s \cdot \hat{\vec{R}}_{qm}} \quad (\text{A4})$$

$$\vec{I}(\vec{R}) = \int_{\text{element}} \vec{I}_{00}(\vec{R}') \left\{ \sum_{q=-\infty}^{\infty} \sum_{m=-\infty}^{\infty} e^{-j\beta s \cdot \vec{R}_{qm}} \delta(\vec{R} - \vec{R}_{qm} - \vec{R}') \right\} d\vec{R}'$$

(A5)

using the properties of the delta function.

The scattered field will be found by solving the differential equation for the vector potential  $\vec{A}(\vec{R})$ :

$$\nabla^2 \vec{A} + \beta^2 \vec{A} = -\mu \vec{I}(\vec{R})$$

(A6)

$$\beta^2 = \omega^2 \mu \epsilon .$$

(A7)

The problem is simplified by considering the scalar equation,

$$(\nabla^2 + \beta^2) G(\vec{R}'') = \mu \left\{ \sum_{q=-\infty}^{\infty} \sum_{m=-\infty}^{\infty} e^{-j\beta s \cdot \vec{R}_{qm}} \delta(\vec{R}'' - \vec{R}_{qm}) \right\} .$$

(A8)

Integrating both sides of this equation by  $\int \vec{I}_{00}(\vec{R}')$  with

$$\vec{R}'' = \vec{R} - \vec{R}'$$

(A9)

gives

$$\vec{A}(\vec{R}) = \int_{\text{element}} \vec{I}_{00}(\vec{R}') G(\vec{R} - \vec{R}') d\vec{R}'$$

(A10)

where  $G(\vec{R}'')$  is the scalar Green's function.

### Evaluating G(R)

The primes in Equation (A8) will be dropped. Let the Fourier transform of  $\vec{G}(\vec{R})$  be defined by

$$F(\vec{\xi}) \equiv \iint_{-\infty}^{\infty} e^{-j\beta \vec{R} \cdot \vec{\xi}} \vec{G}(\vec{R}) d\vec{R}. \quad (A11)$$

Applying the transform to Equation (A8) and substituting Equation (A2) gives

$$\beta^2(1 - \vec{s} \cdot \vec{\xi}) F(\vec{\xi}) = -\mu \left\{ \sum_{q=-\infty}^{\infty} \sum_{m=-\infty}^{\infty} e^{-j\beta(qs_1 + ms_2)} e^{j\beta(q\xi_1 + m\xi_2)} \right\} \quad (A12)$$

where

$$\begin{aligned} s_1 &= \hat{s} \cdot \vec{d}_1 & s_2 &= \hat{s} \cdot \vec{d}_2 \\ \xi_1 &= \vec{\xi} \cdot \vec{d}_1 & \xi_2 &= \vec{\xi} \cdot \vec{d}_2. \end{aligned} \quad (A13)$$

Using the identify

$$\sum_{n=-\infty}^{\infty} e^{jn\omega_0 t} = \frac{2\pi}{\omega_0} \sum_{n=-\infty}^{\infty} \delta(t - n \frac{2\pi}{\omega_0}) \quad (A14)$$

with the substitutions

$$\omega_0 = \beta, t = \xi_1 - s_1, \text{ and } \omega_0 = \beta, t = \xi_2 - s_2 \quad (A15)$$

gives,

$$\sum_{q=-\infty}^{\infty} e^{j\beta q(\xi_1 - s_1)} = \lambda \sum_{k=-\infty}^{\infty} \delta(\xi_1 - (s_1 + k\lambda)) \quad (A16)$$

$$\sum_{m=-\infty}^{\infty} e^{j\beta m(\xi_2 - s_2)} = \lambda \sum_{n=-\infty}^{\infty} \delta(\xi_2 - (s_2 + n\lambda)).$$

Substituting Equations (A16) into Equation (A12) we obtain

$$F(\xi) = \frac{-\mu\lambda^2}{\beta^2} \sum_{k=-\infty}^{\infty} \sum_{n=-\infty}^{\infty} \frac{\delta(\xi_1 - (s_1 + k\lambda)) \delta(\xi_2 - (s_2 + n\lambda))}{1 - \xi \cdot \xi}. \quad (A17)$$

Applying the inverse transform to Equation (A17):

$$G(R) = \frac{-\lambda\mu}{4\pi^2} \iiint_{-\infty}^{\infty} \sum_{k=-\infty}^{\infty} \sum_{n=-\infty}^{\infty} e^{-j\beta R \cdot \xi} \frac{\delta(\xi_1 - (s_1 + k\lambda)) \delta(\xi_2 - (s_2 + n\lambda))}{1 - \xi \cdot \xi} d\xi \quad (A18)$$

So far, only two vector directions have been chosen  $\vec{d}_1$  and  $\vec{d}_2$ . A third independent vector is needed to completely specify any direction in space as a linear combination of these three vectors. We will choose

$$\vec{d}_3 = \vec{d}_1 \times \vec{d}_2 / \|\vec{d}_1 \times \vec{d}_2\|. \quad (A19)$$

This choice provides the greatest simplicity in the resulting equations. With the three (contravariant) vectors  $\vec{d}_1, \vec{d}_2, \vec{d}_3$  specified, we can form the corresponding covectors  $\vec{b}^1, \vec{b}^2, \vec{b}^3$  according to the formula

$$\vec{d}_i \cdot \vec{b}^j = \delta_i^j \quad (A20)$$

$\delta_i^j$  = Kronecker delta.

Equations (A19) and (A20) yield the following equivalent forms:

$$\begin{aligned}\vec{b}^1 &= \vec{d}_2 \times \vec{d}_3 / \|\vec{d}_1 \times \vec{d}_2\| \\ \vec{b}^2 &= \vec{d}_3 \times \vec{d}_1 / \|\vec{d}_1 \times \vec{d}_2\| \\ \vec{b}^3 &= \vec{d}_1.\end{aligned}\quad (A21)$$

Now form a transformation of the integral to the  $(\xi_1, \xi_2, \xi_3)$  system of coordinates where

$$\vec{\xi} = \xi_1 \vec{b}^1 + \xi_2 \vec{b}^2 + \xi_3 \vec{b}^3 \quad (A22)$$

$$\xi_i = \vec{\xi} \cdot \vec{d}_i. \quad (A23)$$

This definition of  $\xi_i$  is consistent with Equations (A13). Under this transform, Equation (A18) becomes,

$$G(\vec{R}) = \frac{-\lambda\mu}{4\pi^2 \|\vec{d}_1 \times \vec{d}_2\|} \sum_{k=-\infty}^{\infty} \sum_{n=-\infty}^{\infty} \iiint_{-\infty}^{\infty} e^{-j\beta(R^1\xi_1 + R^2\xi_2 + R^3\xi_3)} .$$

$$\frac{\delta(\xi_1 - (s_1 + k\lambda)) \delta(\xi_2 - s_2 + n\lambda))}{1 - \frac{\vec{\xi} \cdot \vec{d}}{\|\vec{d}\|}} d\xi_1 d\xi_2 d\xi_3$$

(A24)

$$G(\vec{R}) = \frac{\lambda\mu}{4\pi^2 \|\vec{d}_1 \times \vec{d}_2\|} \sum_{k=-\infty}^{\infty} \sum_{n=-\infty}^{\infty} e^{-j\beta(R^1 r_1 + R^2 r_2)} \int_{-\infty}^{\infty} \frac{e^{-j\beta R^3 \xi_3}}{\xi_3^2 - (1 - \|r_1 \vec{b}^1 + r_2 \vec{b}^2\|^2)} d\xi_3 \quad (A25)$$

with

$$\vec{R} = R^1 \vec{d}_1 + R^2 \vec{d}_2 + R^3 \vec{d}_3 \quad R^i = R \cdot \vec{b}^i \quad (A26)$$

$$r_1 = s_1 + k\lambda \quad (A27)$$

$$r_2 = s_2 + n\lambda .$$

The integral in Equation (A25) is a standard integral often found in oscillating mechanical systems and can be easily evaluated by residues.

$$\int_{-\infty}^{\infty} \frac{e^{-j\beta R^3 \xi_3}}{\xi_3^2 - (1 - \|r_1 \vec{b}^1 + r_2 \vec{b}^2\|^2)} d\xi_3 = \frac{-\pi j}{r_3} e^{\mp j\beta R^3 r_3} \quad (A28)$$

$$\begin{aligned} \text{use } & - \text{ if } R^3 = R \cdot \vec{b}^3 > 0 \\ & + \text{ if } R^3 = R \cdot \vec{b}^3 < 0 \end{aligned}$$

and

$$r_3 = \sqrt{1 - \|r_1 \vec{b}^1 + r_2 \vec{b}^2\|^2} \quad \text{evaluated in 4th quadrant.} \quad (A29)$$

Substituting Equation (A28) into Equation (A25) we obtain,

$$\vec{G}(\vec{R}) = \frac{-j\lambda\mu}{4\pi\|\vec{d}_1 \times \vec{d}_2\|} \sum_{n=-\infty}^{\infty} \sum_{k=-\infty}^{\infty} \frac{e^{-j\beta\vec{R} \cdot \hat{r}_{\pm}}}{r_3} \quad (A30)$$

$$r = r_1 b^1 + r_2 b^2 + r_3 b^3. \quad (A31)$$

Equations (A10) and (A30) now combine to give us the vector potential  $\vec{A}(\vec{R})$  for the planar array:

$$\vec{A}(\vec{R}) = \frac{-j\lambda\mu I(o)}{4\pi\|\vec{d}_1 \times \vec{d}_2\|} \sum_{n=-\infty}^{\infty} \sum_{k=-\infty}^{\infty} \frac{e^{-j\beta\vec{R} \cdot \hat{r}_{\pm}}}{r_3} \hat{P}(\hat{r}_{\pm}) \quad (A32)$$

$$\hat{P}(\hat{r}) \equiv \frac{1}{I(o)} \int_{\text{elements}} I(\vec{r}') e^{j\beta\vec{r} \cdot \vec{R}'} d\vec{r}' . \quad (A33)$$

The subscripts have been dropped from the current and  $I(o)$  refers to the magnitude of the reference current at the origin; this is usually the terminal current. Equation (A33) is the definition of the vector pattern function  $\hat{P}(\hat{r})$ .

### The Electric and Magnetic Fields

The magnetic field is derived from Equation (A32) by

$$\vec{H} = \frac{1}{\mu} \nabla \times \vec{A} \quad (A34)$$

with the vector identity,

$$\nabla \times (\hat{p}f) = \nabla f \times \hat{p} \quad (\hat{p} \text{ is a constant vector}) \quad (A35)$$

which gives

$$\vec{H}(R) = \frac{I(0)}{2\pi d_1 \times d_2} \sum_{n=-\infty}^{\infty} \sum_{k=-\infty}^{\infty} \frac{e^{-j\beta r_{\pm} \cdot R}}{r_3} (\vec{p}(\hat{r}_{\pm}) \times \hat{r}_{\pm}) . \quad (A36)$$

Applying Ampere's equation

$$\vec{E} = \frac{1}{j\omega\epsilon} \nabla \times \vec{H} \quad (A37)$$

and Equation (A35) to Equation (A36) gives

$$\vec{E}(R) = \frac{Z_c I(0)}{2\pi d_1 \times d_2} \sum_{n=-\infty}^{\infty} \sum_{k=-\infty}^{\infty} \frac{e^{-j\beta r_{\pm} \cdot R}}{r_3} [(\vec{p}(\hat{r}_{\pm}) \times \hat{r}_{\pm}) \times \hat{r}_{\pm}] \quad (A38)$$

with,

$$Z_c = \sqrt{\mu/\epsilon} . \quad (A39)$$

when the reference point is located at  $\vec{R}^{(1)}$ ,

$$\vec{E}(R) = \frac{Z_c I(\vec{R}^{(1)})}{2\pi d_1 \times d_2} \sum_{n=-\infty}^{\infty} \sum_{k=-\infty}^{\infty} \frac{e^{-j\beta r_{\pm} \cdot (R-R^{(1)})}}{r_3} [(\vec{p}(\hat{r}_{\pm}) \times \hat{r}_{\pm}) \times \hat{r}_{\pm}] \quad (A40)$$

$$\vec{p}^{(1)}(\hat{r}) = \frac{1}{I(\vec{R}^{(1)})} \int_{\text{element}} I(\vec{R}') e^{j\beta r \cdot R'} d\vec{R}' ; \quad (A41)$$

$\vec{R}'$  is a vector from  $R^{(1)}$  to the integration point.

## APPENDIX B

### PATTERN FACTORS FOR DIPOLES AND LOOPS

In this appendix, pattern factors, vector pattern functions, and current distributions used in the examples will be considered.

For the case of a linear round wire with a current distribution  $I(\ell')$  and direction  $\hat{p}$  shown in Figure B.1, the vector pattern function is defined to be,

$$\hat{P}(\hat{r}) = \frac{\hat{p}}{I(0)} \int_{\text{element}} I(\ell') e^{j\beta R' \cdot \hat{r}} dR' \quad (B1)$$

from Equation (2.4). Therefore,

$$\hat{P}(\hat{r}) = \frac{\hat{p}}{I^f(0)} \frac{1}{2\pi} \int_0^{2\pi} \int_{\ell_1}^{\ell_2} I^f(\ell') e^{j\beta R' \cdot \hat{r}} d\ell' d\phi' \quad (B2)$$

$$\hat{R}' = \ell' \hat{p} + a(\hat{t}_1 \cos\phi + \hat{t}_2 \sin\phi) \quad (B3)$$

where  $(\hat{p}, \hat{t}_1, \hat{t}_2)$  form an orthonormal basis,  $a$  is the wire radius, and  $I^f$  stands for the filamentary current distribution. Separating the integrals gives

$$\hat{P}(\hat{r}) = \hat{p} P(\hat{r}) \left\{ \frac{1}{2\pi} \int_0^{2\pi} e^{j\beta a(r t_1 \cos\phi + r t_2 \sin\phi)} d\phi \right\} \quad (B4)$$

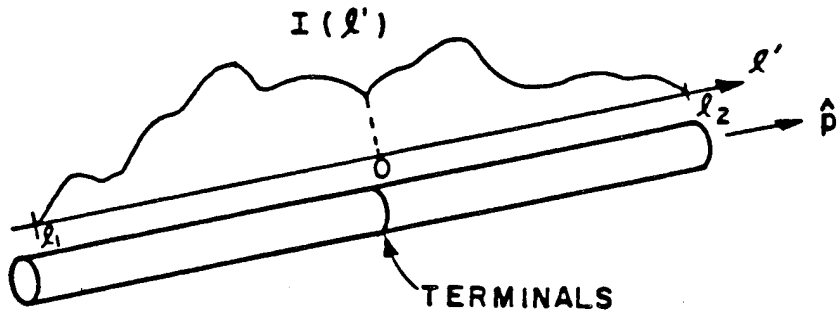


Figure B.1. A linear round wire with a current distribution  $\hat{p}I(l')$ .

$$r_{t_1} = \hat{r} \cdot \hat{t}_1$$

$$r_{t_2} = \hat{r} \cdot \hat{t}_2$$

$$r_p = \hat{r} \cdot \hat{p} \quad (B5)$$

and

$$P(\hat{r}) = \frac{1}{I_f(0)} \int_{l_1}^{l_2} I^f(l') e^{j\beta l' r_p} d l' \quad (B6)$$

is the filamentary pattern factor.

It can be shown from the properties of the Bessel function that

$$J_0(\sqrt{x^2+y^2}) = \frac{1}{2\pi} \int_0^{2\pi} e^{j(x\cos\phi + y\sin\phi)} d\phi. \quad (B7)$$

Therefore,

$$\hat{P}(\hat{r}) = \hat{p}P(\hat{r}) J_0(\beta a \sqrt{r_{t1}^2 + r_{t2}^2}) . \quad (B8)$$

Since  $\hat{r}$  is a unit vector,

$$r_{t1}^2 + r_{t2}^2 + r_p^2 = 1 \quad (B9)$$

and so

$$\hat{P}(\hat{r}) = \hat{p}P(\hat{r}) J_0(\beta a \sqrt{1-r_p^2}) \quad (B10)$$

which is Equation (2.43). Similarly,

$$\hat{P}^t(\hat{r}) = \hat{p}P^t(\hat{r}) J_0(\beta a \sqrt{1-r_p^2}) . \quad (B11)$$

### Dipole Current

The filamentary current distribution on a dipole under scattering conditions is given by

$$I^f(\ell') = (A + B\cos(\beta\ell')) \quad |\ell'| < \ell \quad (B12)$$

illustrated in Figure B.2. The constants A and B are determined by the conditions

$$I(0) = 1$$

$$I^f(\ell_e) = 0$$

$$\ell_e = \ell + \Delta\ell \quad (B13)$$

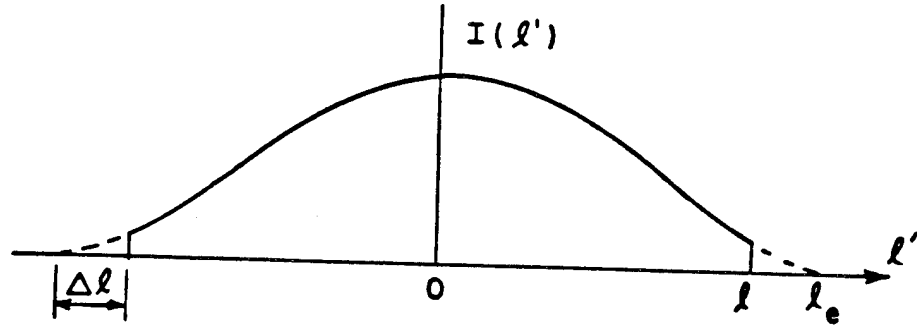


Figure B.2. Scattering (cosine) current distribution on a dipole.

in which  $\Delta l$  is a correction due to end effect capacitances and is set equal to zero in the examples of Chapter III. Equations (B12) and (B13) yield,

$$A = \frac{\cos(\beta l_e)}{\cos(\beta l_e) - 1} \quad (B14)$$

$$B = \frac{1}{1 - \cos(\beta l_e)} . \quad (B15)$$

The scattering current pattern factor is then found to be,

$$P(r_p) = 2A\ell \left[ \frac{\sin(\beta r_p \ell)}{\beta r_p \ell} \right] + \frac{2B}{\beta} \left[ \frac{r_p \cos(\beta \ell) \sin(\beta r_p \ell) - \sin(\beta \ell) \cos(\beta r_p \ell)}{r_p^2 - 1} \right]. \quad (B16)$$

This expression combined with Equation (B10) gives the vector pattern function for a scattering current distribution.

The filamentary current distribution on a dipole under transmitting conditions is,

$$I^f(\ell') = \sin(\beta(\ell_e - |\ell'|)) \quad \text{for } |\ell'| < \ell \quad (B17)$$

illustrated in Figure B.3. The transmitting pattern factor is obtained using Equation (2.46) and yields,

$$P^t(r_p) = \frac{2}{\beta(1-r_p^2)\sin(\beta\ell_e)} \left\{ -\cos(\beta\ell_e) + \cos(\beta\Delta\ell)\cos(\beta r_p \ell) - r_p \sin(\beta\Delta\ell)\sin(\beta r_p \ell) \right\}. \quad (B18)$$

The vector transmitting pattern function is found from Equation (B11).

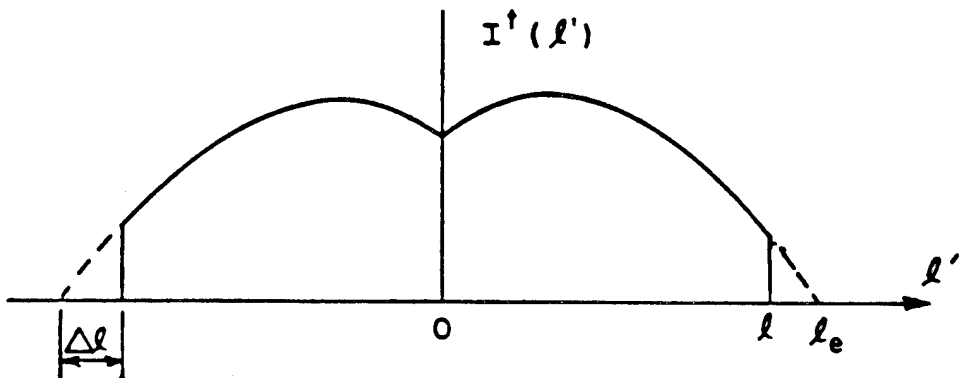


Figure B.3. Transmitting (sine) current distribution on a dipole.

#### Loop Current

The cosine current distribution used by Kent for a rectangular loop is

$$I^f(l') = \frac{\cos(\beta l')}{\cos 2\beta(a+b)} \quad (B19)$$

and is shown in Figure B.4. Each side contributes the following terms to the pattern factor:

$$\begin{aligned} P_1(\hat{r}) \frac{-2}{\beta \cos(\beta c)(1-r_p^2)} & \{ \sin(\beta c) - \cos(\beta r_b b) \sin \beta(c-b) \\ & - r_b \sin(\beta r_b b) \cos(\beta(c-b)) \} \end{aligned} \quad (B20)$$

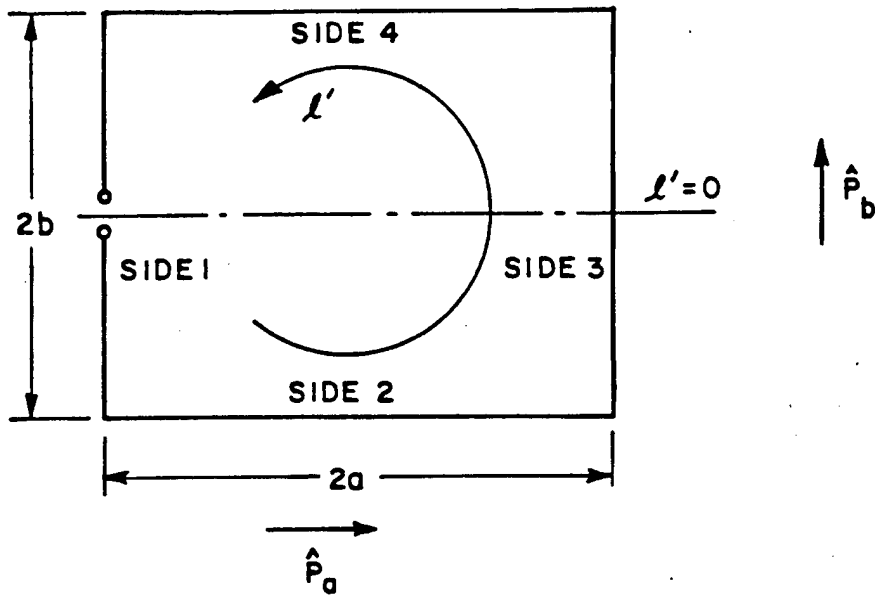


Figure B.4. Rectangular loop antenna.

$$P_3(\hat{r}) \frac{2e^{j\beta a 2r_a}}{\beta \cos(\beta c)(1-r_b^2)} \{ \sin(\beta b) \cos(\beta r_b b) - r_b \sin(\beta r_b b) \cos(\beta b) \}$$

(B21)

$$\begin{aligned} P_2(\hat{r}) + P_4(\hat{r}) &= \frac{2 \sin(\beta b r_b)}{\beta \cos(\beta c)(1-r_a^2)} \{ -r_a \cos(\beta(c-b)) - j \sin(\beta(c-b)) \\ &\quad + r_a e^{j2\beta a r_a} \cos(\beta b) + j e^{j2\beta a r_a} \sin(\beta b) \} \end{aligned} \quad (B22)$$

where

$$c = 2a + 2b$$

$$r_a = \hat{r} \cdot \hat{p}_a$$

$$r_b = \hat{r} \cdot \hat{p}_b .$$

(B23)

The vector pattern function is therefore,

$$\begin{aligned}\hat{\mathbf{P}}(\hat{\mathbf{r}}) = & \left\{ \hat{p}_a J_0(\beta a \sqrt{1-r_a^2}) [P_2(\hat{\mathbf{r}}) + P_4(\hat{\mathbf{r}})] \right. \\ & \left. + \hat{p}_b J_0(\beta b \sqrt{1-r_b^2}) [P_1(\hat{\mathbf{r}}) + P_3(\hat{\mathbf{r}})] \right\} .\end{aligned}\quad (B24)$$

The transmitting vector pattern function is

$$\hat{\mathbf{P}}^t(\hat{\mathbf{r}}) = \hat{\mathbf{P}}(-\hat{\mathbf{r}}) . \quad (B25)$$

## BIBLIOGRAPHY

- [1] English, E.K., "Electromagnetic Scattering from Infinite Periodic Arrays of Arbitrarily Oriented Dipole Elements Imbedded in a General Stratified Medium", Ph.D. Dissertation, The Ohio State University, Columbus, Ohio, 1983.
- [2] Kent, B.M. and B.A. Munk, "Impedance Properties of an Infinite Array of Non-planar Rectangular Loop Antennas Embedded in a General Stratified Medium", Report 715582-3, July 1984, The Ohio State University ElectroScience Laboratory; prepared under Contract No. F33615-83-C-1013 for Aeronautical Systems Division, Wright-Patterson Air Force Base, Ohio.
- [3] Lin, J.S., "On the Scan Impedance of an Array of V-Dipoles and the Effect of the Feed Lines", Ph.D. Dissertation, The Ohio State University, Columbus, Ohio, 1985.
- [4] Ng, K., "Admittance Properties of a Slot Array with Parasitic Wire Arrays in a Stratified Medium", Technical Report 716148-3, January 1985, The Ohio State University ElectroScience Laboratory; prepared under Grant NSG - 1613 for National Aeronautics and Space Administration, Langley Research Center, Virginia.
- [5] Kornbau, T.W., "Application of the Plane Wave Expansion Method to Periodic Arrays Having A Skewed Grid Geometry", Report 4646-3, June 1977, The Ohio State University ElectroScience Laboratory; prepared under Contract No. F33615-76-C-1024 for Air Force Avionics Laboratory, Air Force Wright Aeronautical Laboratories, Wright-Patterson Air Force Base, Ohio.
- [6] Brillouin, L., Wave Propagation in Periodic Structures, Dover Publications, Inc., 1953.
- [7] Munk, B.A., G.A. Burrell, and T.W. Kornbau, "A General Theory of Periodic Surfaces in Stratified Dielectric Media", Technical Report AFAL-TR-77-219, November 1977, Air Force Avionics Laboratory, Air Force Wright Aeronautical Laboratories, Air Force Systems Command, Wright-Patterson Air Force Base, Ohio.
- [8] Koch, W.E., "Metallic Delay Lenses", Bell System Technical Journal, Vol. 27, p. 58, 1948.